

# Analytic results for scalar-mediated Higgs boson production in association with two jets

---

Lucy Budge,<sup>a</sup> John M. Campbell,<sup>b</sup> R. Keith Ellis,<sup>a</sup> Satyajit Seth<sup>c</sup>

<sup>a</sup>*Institute for Particle Physics Phenomenology, Durham University, Durham, DH1 3LE, UK*

<sup>b</sup>*Fermilab, PO Box 500, Batavia IL 60510-5011, USA*

<sup>c</sup>*Physical Research Laboratory, Navrangpura, Ahmedabad - 380009, India*

*E-mail:* [lucy.budge@durham.ac.uk](mailto:lucy.budge@durham.ac.uk), [johnmc@fnal.gov](mailto:johnmc@fnal.gov), [keith.ellis@durham.ac.uk](mailto:keith.ellis@durham.ac.uk), [seth@prl.res.in](mailto:seth@prl.res.in)

**ABSTRACT:** We present compact analytic formulae for all one-loop amplitudes representing the production of a Higgs boson in association with two jets, mediated by a colour triplet scalar particle. Many of the integral coefficients present for scalar mediators are identical to the case when a massive fermion circulates in the loop, reflecting a close relationship between the two theories. The calculation is used to study Higgs boson production in association with two jets in a simplified supersymmetry (SUSY) scenario in which the dominant additional contributions arise from loops of top squarks. The results presented here facilitate an indirect search for top squarks in this channel, by a precision measurement of the corresponding cross-section. However, we find that the potential for improved discrimination between the SM and SUSY cases suggested by the pattern of results in the 1- and 2-jet samples is unlikely to be realized due to the loss in statistical power compared to an inclusive analysis.

---

## Contents

<b>1</b>	<b>Introduction</b>	<b>1</b>
<b>2</b>	<b>Setup</b>	<b>2</b>
<b>3</b>	<b>Calculation of Higgs+2 jet process</b>	<b>5</b>
<b>4</b>	<b>Four-parton integral coefficients for a scalar loop</b>	<b>8</b>
<b>5</b>	<b>Recap of inclusive and 1-jet results</b>	<b>19</b>
<b>6</b>	<b>Results for the 2-jet process</b>	<b>24</b>
<b>7</b>	<b>Conclusions</b>	<b>27</b>
<b>A</b>	<b>Numerical value of coefficients at a given phase-space point</b>	<b>29</b>
<b>B</b>	<b>Large mass limit</b>	<b>29</b>

---

## 1 Introduction

The main production channel of Higgs bosons at the Large Hadron Collider (LHC) is through gluon-gluon fusion *i.e.*,  $gg \rightarrow h$ . The leading order process starts at one loop, mediated by massive quark(s) of the Standard Model (SM). By marrying high-quality data from run 2 of the LHC with precision theoretical calculations for this process [1, 2], one can extract ever more exquisite determinations of the properties of the Higgs boson [3, 4].

As more data is collected, additional information can be obtained from analyzing differential information beyond inclusive cross sections. One reason this is important is that additional jet activity allows new kinematic regions to be examined that may be more sensitive probes of Higgs properties. An example of this is that the nature of the Higgs coupling to particles circulating in the loop can only be probed if the relevant energy scale is at least of order of the particle’s mass. For inclusive production the relevant energy scale is the Higgs mass and, since  $m_h < m_t$ , one can describe this process using an effective field theory (EFT) in which the loop of heavy top quarks is replaced by an effective Lagrangian,

$$\mathcal{L}_{\text{eff}} = \frac{g_s^2}{48\pi^2 v} h G_{\mu\nu}^A G^{A,\mu\nu}, \quad (1.1)$$

where  $g_s$  is the strong coupling constant,  $v$  is the vacuum expectation value of the Higgs field,  $G_{\mu\nu}$  is the QCD field strength, and  $h$  is the Higgs boson field. Indeed, the efficacy of this approximation is the very reason that such high-precision calculations of this process can be performed [1, 2]. In the presence of additional jet activity the relevant energy scale is no longer  $m_h$  but is instead the transverse momentum ( $p_T$ ) of the leading jet. Therefore the Higgs+jet process can become especially sensitive to the coupling of the Higgs boson to new mediator particles of mass  $m_X$  once  $p_T > m_X$ .

An analysis of the cross section for this process, in this kinematic regime, could thus provide the first signal of new physics (in the case of a deviation from the SM prediction), or a stringent bound on the mass and coupling of any new mediator particle. Although less sensitive than corresponding direct searches, such indirect probes of the mediator particles are insensitive to any assumptions regarding the nature of their decay chains and may therefore provide complementary information.

Massive colour triplet scalar particles that arise in beyond the Standard Model (BSM) scenarios, are potential new mediators for couplings of gluons to the Higgs boson. Indeed, one of the main goals of the LHC is to further explore the particles to which the Higgs boson couples, and having already discovered one fundamental scalar particle it is natural to consider whether further scalar degrees of freedom might exist. One such proposed scalar particle is the top squark, a super partner of the SM top quark that appears in the Minimal Supersymmetric Standard Model (MSSM). The effect of such loops of particles has been explored previously [5–7], focussing on effects in either inclusive Higgs production or in the case of the Higgs boson recoiling against a single jet. Most recently, Ref. [8] demonstrated that the 1-jet process offers, in principle, superior information to inclusive production over certain regions of parameter space. For the top squark, current indirect limits from Higgs and electroweak data [9, 10] are around  $m_{\tilde{t}} \sim 300$  GeV. As noted above, this limit is clearly much weaker than any direct limit derived from a specific decay chain, which is currently around the 1 TeV scale (see, for example, Refs. [11] and [12] for recent limits from CMS and ATLAS).

In this paper we will extend this analysis to the case in which a Higgs boson is produced in association with two jets. To do so we have performed a new calculation of the amplitudes for the scattering of a Higgs boson with four partons, mediated by a loop of coloured scalar particles. Our results are expressed in the form of compact analytic expressions, exploiting a close correspondence with their fermionic counterparts [13]. The resulting expressions may be evaluated numerically in a fast and stable manner, allowing for the construction of an efficient Monte Carlo event generator. We first outline the generic scalar theory in which we shall perform our calculation, as well as the specific MSSM case, in section 2. The computation of the four-parton matrix elements entering the Higgs+2 jet analysis is given in section 3, with results for one-loop integral coefficients for the case of a scalar loop detailed in section 4. We move to phenomenology in section 5, first providing a recalculation and recap of results for the 0- and 1-jet cases before presenting our new 2-jet analysis in section 6. Our conclusions are drawn in section 7. Finally, as an aid to performing an independent implementation of the formulae presented here, appendix A provides numerical results for the integral coefficients given in section 4, and appendix B details the connection between our amplitudes and those obtained in the EFT.

## 2 Setup

We first formulate a generic scalar theory involving a complex scalar  $\phi$  which carries  $SU(3)$  colour in the triplet representation. The Lagrangian involving  $\phi$  thus reads,

$$\mathcal{L} = (D^\mu \phi_i^\dagger)(D_\mu \phi_i) - \lambda \phi_i^\dagger \phi_i h, \quad D_\mu \phi_i = \partial_\mu \phi_i + i \frac{g_s}{\sqrt{2}} (t \cdot \mathcal{G}_\mu)_{ij} \phi_j, \quad (2.1)$$

where  $\mathcal{G}_\mu^a$  denotes the gluon field,  $t^a$  represents the standard  $SU(3)$  colour generators, normalized such that  $\text{tr}(t^a t^b) = \delta^{ab}$  and  $g_s$  is the strong coupling constant. The coupling of the Higgs boson to the scalar field is denoted by the parameter  $\lambda$ .

## 2.1 Overview

In order to elucidate the differences – and similarities – between the cases of Higgs boson production mediated by a fermion and a scalar loop, we first examine the amplitudes for inclusive Higgs boson production via these two processes.

In the Standard Model, where the particle in the loop is a quark of mass  $m$ , the amplitude for  $g(p_1)g(p_2) \rightarrow h$  takes the following form,

$$\mathcal{H}_2^{gg} = i \frac{g_s^2}{16\pi^2} \delta^{AB} \left( \frac{m^2}{v} \right) \left[ g^{\mu\nu} - \frac{p_1^\nu p_2^\mu}{p_1 \cdot p_2} \right] \left[ (2m_h^2 - 8m^2) C_0(p_1, p_2; m) - 4 \right] \epsilon_\mu(p_1) \epsilon_\nu(p_2). \quad (2.2)$$

The gluons have colour labels  $A$  and  $B$ ,  $\epsilon$  represents a polarization vector, and  $m_h$  denotes the mass of the Higgs boson. The integral over the loop momentum is encapsulated in the scalar triangle function  $C_0(p_1, p_2, m)$  defined later in Eq. (3.7). The corresponding result for a loop containing a scalar particle of mass  $m$  is [14],

$$\mathcal{A}_2^{gg} = i \frac{g_s^2}{16\pi^2} \delta^{AB} \left( \frac{-\lambda}{4} \right) \left[ g^{\mu\nu} - \frac{p_1^\nu p_2^\mu}{p_1 \cdot p_2} \right] \left[ -8m^2 C_0(p_1, p_2; m) - 4 \right] \epsilon_\mu(p_1) \epsilon_\nu(p_2). \quad (2.3)$$

Writing the amplitudes in this way highlights several similarities between them. When setting  $(-\lambda/4) = m^2/v$  the coefficient of the triangle integral proportional to  $m^2$  is identical, as well as the purely rational term  $(-4)$ . This illustrates a general correspondence between such coefficients in the scalar and fermion theories [13].

It is instructive to push this comparison further by extracting an overall factor as follows,

$$\begin{aligned} \mathcal{H}_2^{gg} &= i \frac{g_s^2}{16\pi^2} \delta^{AB} \left[ \frac{1}{2} \left( g^{\mu\nu} - \frac{p_1^\nu p_2^\mu}{p_1 \cdot p_2} \right) \right] \left( \frac{m_h^2}{v} \right) \epsilon_\mu(p_1) \epsilon_\nu(p_2) F_{1/2}(\tau), \\ \mathcal{A}_2^{gg} &= i \frac{g_s^2}{16\pi^2} \delta^{AB} \left[ \frac{1}{2} \left( g^{\mu\nu} - \frac{p_1^\nu p_2^\mu}{p_1 \cdot p_2} \right) \right] \left( \frac{\lambda m_h^2}{2m^2} \right) \epsilon_\mu(p_1) \epsilon_\nu(p_2) F_0(\tau), \end{aligned} \quad (2.4)$$

where the functions for the scalar and fermionic cases are given by,

$$F_0(\tau) = \tau [1 - \tau f(\tau)], \quad (2.5)$$

$$F_{1/2}(\tau) = -2\tau [1 + (1 - \tau)f(\tau)], \quad F_{1/2}(\tau) = -2F_0(\tau) - 2\tau f(\tau), \quad (2.6)$$

and  $\tau = 4m^2/m_h^2$ . In these formulae we have introduced the triangle function  $f(\tau) = -\frac{m_h^2}{2} C_0(p_1, p_2; m)$ , for which the explicit result is,

$$f(\tau) = -\frac{1}{4} \theta(1 - \tau) \left[ \ln \left( \frac{1 + \sqrt{1 - \tau}}{1 - \sqrt{1 - \tau}} \right) - i\pi \right]^2 + \theta(\tau - 1) [\sin^{-1}(1/\sqrt{\tau})]^2. \quad (2.7)$$

Figure 1 shows the behaviour of  $F_0$  and  $F_{1/2}$  as a function of  $\tau$ . In the region  $\tau > 1$  the functions are both real and both negative, and quickly approach their asymptotic values of  $-1/3$  (scalar) and  $-4/3$  (fermion). For the SM case  $\tau \gg 1$  and the value of this function is in the asymptotic regime, motivating the use of the EFT shown in Eq. (1.1). From these asymptotic values and the overall factors extracted in Eqs.(2.6) and (2.5) it is clear that the two processes can be described by the same effective Lagrangian, in the limit of large intermediary mass, when we have  $(\lambda/8) = m^2/v$ .

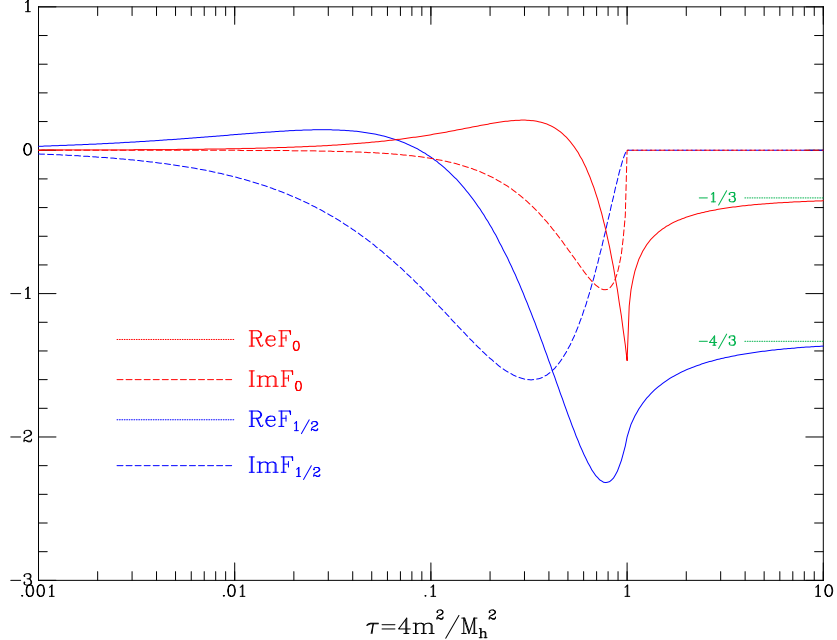


**Figure 1.** The functions  $F_{1/2}$  and  $F_0$ , given in Eqs. (2.6) and (2.5) respectively, plotted as a function of their arguments. The (green) dashed lines show their asymptotes at large  $\tau$ .

## 2.2 Top squarks in the MSSM

Although the analytic results presented later in this paper are valid for a generic color-triplet scalar, and may be applicable more generally, in this paper we will focus on the top squark sector of the MSSM, which contains two such scalars,  $\tilde{t}_1$  and  $\tilde{t}_2$ . We will consider scenarios in which the coupling of the lightest Higgs boson in the MSSM is modified, assuming that this corresponds to the particle already observed at the LHC. Each squark couples to the lightest Higgs boson through a contribution to the Lagrangian of the form shown in Eq. (2.1), where we now label the strength of the Higgs coupling to each scalar by  $\lambda_{h\tilde{t}_1\tilde{t}_1}$  and  $\lambda_{h\tilde{t}_2\tilde{t}_2}$  respectively. Following ref. [8] we parametrize this sector by,

$$(m_{\tilde{t}_1}, \Delta m, \theta), \quad \Delta m = \sqrt{m_{\tilde{t}_2}^2 - m_{\tilde{t}_1}^2}, \quad (2.8)$$

where, rather than using the two squark masses, we use the lightest top squark mass ( $m_{\tilde{t}_1}$ ) and a measure of the separation with the other state ( $\Delta m$ ). The final parameter ( $\theta$ ) is the mixing angle between the two scalar states, which takes values in the range  $[-\pi/2, \pi/2]$ . If the mass of the MSSM pseudoscalar ( $A$ ) is much larger than the weak scale ( $m_A \gg m_Z$ ) we can work in the decoupling limit [15], in which the Higgs-squark couplings take a very simple form:

$$\lambda_{h\tilde{t}_1\tilde{t}_1} = \frac{m_t^2}{v} \left( \alpha_1 \cos^2 \theta + \alpha_2 \sin^2 \theta + 2 - \frac{(\Delta m)^2}{2m_t^2} \sin^2 2\theta \right), \quad (2.9)$$

$$\lambda_{h\tilde{t}_2\tilde{t}_2} = \frac{m_t^2}{v} \left( \alpha_1 \sin^2 \theta + \alpha_2 \cos^2 \theta + 2 + \frac{(\Delta m)^2}{2m_t^2} \sin^2 2\theta \right). \quad (2.10)$$

The coefficients  $\alpha_1$  and  $\alpha_2$  in these formulae are given by,

$$\alpha_1 = \frac{m_Z^2}{m_t^2} \cos 2\beta \left( 1 - \frac{4}{3} \sin^2 \theta_W \right), \quad (2.11)$$

$$\alpha_2 = \frac{4}{3} \frac{m_Z^2}{m_t^2} \cos 2\beta \sin^2 \theta_W, \quad (2.12)$$

where  $\theta_W$  is the weak mixing angle. These formulae also contain the final MSSM parameter that is necessary to specify our model,  $\beta$ , where  $\tan \beta$  is the ratio of the vacuum expectation value of the two Higgs bosons.

### 3 Calculation of Higgs+2 jet process

We now provide the details of our calculation of the four-parton amplitudes that enter our analysis of the Higgs+2 jet process.

#### 3.1 Amplitudes for a scalar loop

We begin with the Lagrangian given in Eq. (2.1) and break the amplitude for the production of a Higgs boson and  $n$  gluons, mediated by a scalar loop, into colour-ordered sub-amplitudes. Following the notation of Ref. [13] we have,

$$\mathcal{A}_n^{gggg}(\{p_i, h_i, c_i\}) = i \frac{g_s^n}{16\pi^2} \left( -\frac{\lambda}{4} \right) \sum_{\{1,2,\dots,n\}'} \text{tr}(t^{c_1} t^{c_2} \dots t^{c_n}) A_n^{\{c_i\}}(1^{h_1}, 2^{h_2}, \dots, n^{h_n}; h), \quad (3.1)$$

where the sum with the *prime*,  $\sum_{\{1,2,\dots,n\}'}$ , is over all  $(n-1)!$  *non-cyclic* permutations of  $1, 2, \dots, n$ ,  $\lambda$  is the Higgs-scalar-scalar coupling and the  $t$  matrices are the SU(3) matrices in the fundamental representation normalized such that,

$$\text{tr}(t^a t^b) = \delta^{ab}. \quad (3.2)$$

$m$  is the mass of the scalar circulating in the loop. It is sufficient to calculate one permutation in this sum, with the other colour sub-amplitudes related by Bose symmetry and obtained by exchange. The explicit result for the four gluon case is,

$$\begin{aligned} \mathcal{A}_4^{gggg}(\{p_i, h_i, c_i\}) = & i \frac{g_s^4}{16\pi^2} \left( -\frac{\lambda}{4} \right) \left\{ [\text{tr}(t^{c_1} t^{c_2} t^{c_3} t^{c_4}) + \text{tr}(t^{c_1} t^{c_4} t^{c_3} t^{c_2})] A_4^{1234}(1^{h_1}, 2^{h_2}, 3^{h_3}, 4^{h_4}; h) \right. \\ & + [\text{tr}(t^{c_1} t^{c_3} t^{c_4} t^{c_2}) + \text{tr}(t^{c_1} t^{c_2} t^{c_4} t^{c_3})] A_4^{1342}(1^{h_1}, 2^{h_2}, 3^{h_3}, 4^{h_4}; h) \\ & \left. + [\text{tr}(t^{c_1} t^{c_4} t^{c_2} t^{c_3}) + \text{tr}(t^{c_1} t^{c_3} t^{c_2} t^{c_4})] A_4^{1423}(1^{h_1}, 2^{h_2}, 3^{h_3}, 4^{h_4}; h) \right\}. \quad (3.3) \end{aligned}$$

We also need the amplitude for the production of a Higgs boson, an antiquark, quark and two gluons. It can be similarly decomposed into colour-ordered amplitudes as follows.

$$\begin{aligned} \mathcal{A}_4^{\bar{q}qgg}(\{p_i, h_i, c_i, j_i\}) = & i \frac{g_s^4}{16\pi^2} \left( -\frac{\lambda}{4} \right) \left[ (t^{c_3} t^{c_4})_{j_2 j_1} A_4^{34}(1^{h_1}, 2^{-h_1}, 3^{h_3}, 4^{h_4}; h) \right. \\ & \left. + (t^{c_4} t^{c_3})_{j_2 j_1} A_4^{43}(1^{h_1}, 2^{-h_1}, 3^{h_3}, 4^{h_4}; h) \right]. \quad (3.4) \end{aligned}$$

The colour structure  $\delta^{c_3 c_4} \delta_{j_2 j_1} / N$  is also present in individual diagrams but makes no net contribution to the one-loop amplitude. Here we will give results for the colour-ordered amplitude  $A_4^{34}$  since it is

straightforward to obtain  $A_4^{43}$  from this through the parity operation (complex conjugation) and permutation of momentum labels.

The four-quark amplitude takes the form,

$$\mathcal{A}_4^{4q}(\{p_i, h_i, j_i\}) = i \frac{g_s^4}{16\pi^2} \left( \frac{-\lambda}{4} \right) (t^{c_1})_{j_2 j_1} (t^{c_1})_{j_4 j_3} A_4^{4q}(1_{\bar{q}}^{h_1}, 2_q^{-h_1}, 3_{\bar{q}'}^{h_3}, 4_{q'}^{-h_3}), \quad (3.5)$$

where the helicities of the quarks are fixed by those of the antiquarks.

All colour subamplitudes are then decomposed in terms of scalar integrals. For instance, for the Higgs + 4 gluon case we have,

$$\begin{aligned} A_4^{1234}(1^{h_1}, 2^{h_2}, 3^{h_3}, 4^{h_4}; h) &= \frac{\bar{\mu}^{4-n}}{r_\Gamma} \frac{1}{i\pi^{n/2}} \int d^n \ell \frac{\text{Num}(\ell)}{\prod_i d_i(\ell)} \\ &= \sum_{i,j,k} \tilde{d}_{i \times j \times k}(1^{h_1}, 2^{h_2}, 3^{h_3}, 4^{h_4}) D_0(p_i, p_j, p_k; m) \\ &\quad + \sum_{i,j} \tilde{c}_{i \times j}(1^{h_1}, 2^{h_2}, 3^{h_3}, 4^{h_4}) C_0(p_i, p_j; m) \\ &\quad + \sum_i \tilde{b}_i(1^{h_1}, 2^{h_2}, 3^{h_3}, 4^{h_4}) B_0(p_i; m) + \tilde{r}(1^{h_1}, 2^{h_2}, 3^{h_3}, 4^{h_4}). \end{aligned} \quad (3.6)$$

$\tilde{r}$  are the rational terms and the sums in the above equations scan over groupings of external gluons. The scalar bubble ( $B_0$ ), triangle ( $C_0$ ) and box ( $D_0$ ) integrals are defined by,

$$\begin{aligned} B_0(p_1; m) &= \frac{\bar{\mu}^{4-n}}{r_\Gamma} \frac{1}{i\pi^{n/2}} \int d^n \ell \frac{1}{D(\ell)D(\ell_1)}, \\ C_0(p_1, p_2; m) &= \frac{1}{i\pi^2} \int d^4 \ell \frac{1}{D(\ell)D(\ell_1)D(\ell_{12})}, \\ D_0(p_1, p_2, p_3; m) &= \frac{1}{i\pi^2} \int d^4 \ell \frac{1}{D(\ell)D(\ell_1)D(\ell_{12})D(\ell_{123})}, \\ E_0(p_1, p_2, p_3, p_4; m) &= \frac{1}{i\pi^2} \int d^4 \ell \frac{1}{D(\ell)D(\ell_1)D(\ell_{12})D(\ell_{123})D(\ell_{1234})}, \end{aligned} \quad (3.7)$$

where the denominators are defined as

$$D(\ell) = \ell^2 - m^2 + i\varepsilon, \quad (3.8)$$

and the propagator momenta are,

$$\begin{aligned} \ell_1 &= \ell + p_1 = \ell + q_1, \\ \ell_{12} &= \ell + p_1 + p_2 = \ell + q_2, \\ \ell_{123} &= \ell + p_1 + p_2 + p_3 = \ell + q_3, \\ \ell_{1234} &= \ell + p_1 + p_2 + p_3 + p_4 = \ell + q_4. \end{aligned} \quad (3.9)$$

Finally,  $r_\Gamma = 1/\Gamma(1 - \epsilon) + O(\epsilon^3)$  and  $\bar{\mu}$  is an arbitrary mass scale.

As explained in Ref. [13], we have chosen to work in a basis without pentagon integrals. Nevertheless, we are left with some vestiges of their presence through pentagon-to-box reduction coefficients,

$\mathcal{C}_{1 \times 2 \times 3 \times 4}^{(i)}$ . These can be written as,

$$\begin{aligned}
\mathcal{C}_{1 \times 2 \times 3 \times 4}^{(1)} &= -\frac{1}{2} \frac{s_{23} s_{34} [2 s_{12} s_{24} + s_{13} s_{24} + s_{34} s_{12} - s_{23} s_{14}]}{16 |S_{1 \times 2 \times 3 \times 4}|}, \\
\mathcal{C}_{1 \times 2 \times 3 \times 4}^{(2)} &= -\frac{1}{2} \frac{s_{34} [s_{1234} s_{23} (s_{123} - 2 s_{12}) + s_{123} (s_{34} (s_{123} - s_{23}) + s_{12} (s_{234} + s_{23}) - s_{234} s_{123})]}{16 |S_{1 \times 2 \times 3 \times 4}|}, \\
\mathcal{C}_{1 \times 2 \times 3 \times 4}^{(3)} &= -\frac{1}{2} \frac{[s_{14} s_{23} - (s_{12} + s_{13}) (s_{24} + s_{34})] [s_{34} s_{12} + s_{23} s_{14} - s_{13} s_{24}]}{16 |S_{1 \times 2 \times 3 \times 4}|}, \\
\mathcal{C}_{1 \times 2 \times 3 \times 4}^{(4)} &= -\frac{1}{2} \frac{s_{12} [s_{1234} s_{23} (s_{234} - 2 s_{34}) + s_{234} (s_{12} (s_{234} - s_{23}) + s_{34} (s_{123} + s_{23}) - s_{234} s_{123})]}{16 |S_{1 \times 2 \times 3 \times 4}|}, \\
\mathcal{C}_{1 \times 2 \times 3 \times 4}^{(5)} &= -\frac{1}{2} \frac{s_{12} s_{23} [2 s_{34} s_{13} + s_{13} s_{24} + s_{34} s_{12} - s_{23} s_{14}]}{16 |S_{1 \times 2 \times 3 \times 4}|}. \tag{3.10}
\end{aligned}$$

The denominator factor  $|S_{1 \times 2 \times 3 \times 4}|$  is the determinant of the matrix,  $[S_{1 \times 2 \times 3 \times 4}]_{ij} = [m^2 - \frac{1}{2}(q_{i-1} - q_{j-1})^2]$ , where  $q_i$  is the offset momentum, see Eq. (3.9). It is given by,

$$\begin{aligned}
16 |S_{1 \times 2 \times 3 \times 4}| &= s_{12} s_{23} s_{34} (s_{14} s_{23} - (s_{12} + s_{13}) (s_{24} + s_{34})) + m^2 G, \\
G &= (s_{12} s_{34} - s_{13} s_{24} - s_{14} s_{23})^2 - 4 s_{13} s_{14} s_{23} s_{24}. \tag{3.11}
\end{aligned}$$

We use unitarity techniques to isolate the contribution of boxes [16], triangles [17] and bubbles [18–20]. Pentagon contributions to box coefficients are isolated by applying generalised unitarity cuts on five propagators in  $d = (4 - 2\epsilon)$ -dimensions, with subsequent modification as necessary to remove unphysical singularities and improve numerical stability [13]. The coefficients of each integral are subsequently simplified using the techniques of momentum twistors [21–24] and high precision floating-point arithmetic [25]. We exploit previous results obtained in the calculation of the same processes mediated by a fermion loop [13], noting that for our normalization the coefficients of bubble integrals, some triangle integrals, and the rational part are identical. The results of our analytic calculation of the amplitudes are presented in full in section 4.

### 3.2 Squared matrix elements for fermion and scalar loops

With the scalar-mediated amplitude calculations in hand, we can now describe the calculation of the matrix elements relevant for the MSSM scenario described in Section 2.2. For simplicity and practicality we will include only a top-quark loop in the SM calculation, although the inclusion of a bottom quark loop is straightforward. We can write the subamplitude for a  $n$ -parton process mediated by the top-quark,  $\tilde{t}_1$  and  $\tilde{t}_2$  as,

$$M_n^x = \left(\frac{m_t^2}{v}\right) H_n^x(m_t) - \left(\frac{\lambda_{h\tilde{t}_1\tilde{t}_1}}{4}\right) A_n^x(m_{\tilde{t}_1}) - \left(\frac{\lambda_{h\tilde{t}_2\tilde{t}_2}}{4}\right) A_n^x(m_{\tilde{t}_2}). \tag{3.12}$$

Note that we have taken care to label the mass-dependence of the individual fermion and scalar subamplitudes, and this formula applies to any of the subamplitudes, e.g.  $x = 1234$  ( $gggg$ ),  $x = 34$  ( $\bar{q}qq$ ) or  $x = 4q$  ( $\bar{q}q\bar{q}q$ ). Expressions for all the relevant fermion-mediated subamplitudes  $H_n^x$  are given in Ref. [13].

We can now form the squared matrix elements used in our calculation. For the four-gluon case

we can square the amplitude for a fixed helicity configuration and sum over colours to find,

$$\begin{aligned} \sum_{\text{colours}} |\mathcal{M}_4^{gggg}|^2 &= \left( \frac{g_s^4}{16\pi^2} \right)^2 (N^2 - 1) \left\{ 2N^2 (|M_4^{1234}|^2 + |M_4^{1342}|^2 + |M_4^{1423}|^2) \right. \\ &\quad \left. - 4 \frac{(N^2 - 3)}{N^2} |M_4^{1234} + M_4^{1342} + M_4^{1423}|^2 \right\}, \end{aligned} \quad (3.13)$$

where  $N$  is the dimensionality of the  $SU(N)$  colour group, i.e.  $N = 3$ , and the labels for the helicity configuration (as explicitly shown in Eq. (3.3)) have been suppressed.

Squaring the  $\bar{q}qgg$  amplitude and summing over colours yields,

$$\sum |\mathcal{M}_4^{\bar{q}qgg}|^2 = \left( \frac{g_s^4}{16\pi^2} \right)^2 (N^2 - 1) \left[ N (|M_4^{34}|^2 + |M_4^{43}|^2) - \frac{1}{N} |M_4^{34} + M_4^{43}|^2 \right], \quad (3.14)$$

where the labelling of the helicity configuration shown in Eq. (3.4) has again been suppressed.

Squaring and summing the four-quark amplitude over colours gives,

$$\sum |\mathcal{M}_4^{4q}(h_1, h_3)|^2 = \left( \frac{g_s^4}{16\pi^2} \right)^2 (N^2 - 1) |M_4^{4q}(h_1, h_3)|^2, \quad (3.15)$$

when the quark lines have different flavours. For the case of identical quarks the sum over colours gives,

$$\begin{aligned} \sum |\mathcal{M}_4^{4q}|^2 &= \left( \frac{g_s^4}{16\pi^2} \right)^2 (N^2 - 1) \left( |M_4^{4q}(h_1, h_3)|^2 + |M_4^{4q'}(h_1, h_3)|^2 \right. \\ &\quad \left. + \frac{\delta_{h_1 h_3}}{N} (M_4^{4q}(h_1, h_3) M_4^{4q'}(h_1, h_3)^* + M_4^{4q}(h_1, h_3)^* M_4^{4q'}(h_1, h_3)) \right), \end{aligned} \quad (3.16)$$

where, as indicated, the term on the second line only contributes for quarks of the same helicity and we have introduced,

$$M_4^{4q'}(h_1, h_3) = M_4^{4q}(1_q^{h_1}, 4_q^{-h_1}, 3_q^{h_3}, 2_q^{-h_3}). \quad (3.17)$$

## 4 Four-parton integral coefficients for a scalar loop

In this section we provide expressions for all the box, triangle and bubble coefficients that can be treated as a minimal independent set for Higgs plus four parton helicity amplitudes mediated by a massive scalar. Additional coefficients that can be obtained by momenta permutations and/or helicity flips are tabulated appropriately. As already noted, some of the coefficients are identical to the case when the circulating particle is a massive fermion [13]. Specifically, these are:

- the entire rational contribution,  $\tilde{r}$
- bubble coefficients,  $\tilde{b}_i$
- a subset of triangle coefficients,  $\tilde{c}_i$ , where  $i$  labels all triangles where none of the external legs corresponds to the momentum of the Higgs boson
- the  $m^2$ -dependent term in all triangle coefficients,  $\tilde{c}_i^{(2)}$  (where, in general, we expand  $\tilde{c}_i = \tilde{c}_i^{(0)} + \tilde{c}_i^{(2)} m^2$ )

Expressions for such coefficients are not given here explicitly. Instead we refer to the equation numbers in ref. [13] where they have already been reported. When the expressions for the whole coefficient coincide, these references are appended (inside brackets) in subsequent tables. For the partial coefficients,  $\tilde{c}_i^{(2)}$ , these references are included in the text.

As an aid to implementing these formulae in a numerical code, in appendix A we provide values for all of the coefficients provided here, when evaluated at a specific phase space point. We also give the numerical values of the finite parts of the full amplitudes, obtained by combining these coefficients with an evaluation of all loop integrals according to Eq. (3.6) (and its generalization to all partonic channels).

An additional check of the results presented here is that, in the limit of large mediator mass, all the amplitudes should match onto limiting forms obtained by an explicit calculation in the EFT. This equivalence is spelled-out explicitly in appendix B.

#### 4.1 Coefficients for $A_4^{1234}(g^+, g^+, g^+, g^+; h)$

For the case with four gluons of positive helicity the complete result can easily be written in a form that includes a term proportional to the pentagon scalar integral ( $E_0$ ),

$$\begin{aligned}
A_4(h; 1_g^+, 2_g^+, 3_g^+, 4_g^+) &= \left\{ \frac{4m^2}{\langle 12 \rangle \langle 23 \rangle \langle 34 \rangle \langle 41 \rangle} \left[ -\text{tr}_+ \{1234\} m^2 E_0(p_1, p_2, p_3, p_4; m) \right. \right. \\
&\quad + \frac{1}{2} ((s_{12} + s_{13})(s_{24} + s_{34}) - s_{14}s_{23}) D_0(p_1, p_{23}, p_4; m) \\
&\quad + \frac{1}{2} s_{12}s_{23} D_0(p_1, p_2, p_3; m) \\
&\quad \left. \left. + (s_{12} + s_{13} + s_{14}) C_0(p_1, p_{234}; m) \right] + 2 \frac{s_{12} + s_{13} + s_{14}}{\langle 12 \rangle \langle 23 \rangle \langle 34 \rangle \langle 41 \rangle} \right\} \\
&\quad + \left\{ 3 \text{ cyclic permutations} \right\}. \tag{4.1}
\end{aligned}$$

However, for consistency with the rest of our results and ease of implementation in a numerical code, we prefer to present this result in terms of only box, triangle and bubble coefficients. The box coefficients then take a very simple form when written in terms of the effective pentagon coefficient (obtained by calculating the pentagon coefficient in  $d$  dimensions and taking the  $\mu^2 \rightarrow 0$  limit),

$$\tilde{e}_{1 \times 2 \times 3 \times 4}(1^+, 2^+, 3^+, 4^+) = -4m^4 \frac{\text{tr}_+ \{1234\}}{\langle 12 \rangle \langle 23 \rangle \langle 34 \rangle \langle 41 \rangle} = -4m^4 \frac{[12][34]}{\langle 12 \rangle \langle 34 \rangle}. \tag{4.2}$$

The minimal set of integral coefficients needed to reconstruct the amplitude for this approach is given in the first and third columns of Table 1.

##### 4.1.1 $\tilde{d}_{1 \times 2 \times 34}$

$$\tilde{d}_{1 \times 2 \times 34} = C_{1 \times 2 \times 3 \times 4}^{(4)} \tilde{e}_{\{1^+ \times 2^+ \times 3^+ \times 4^+\}}. \tag{4.3}$$

##### 4.1.2 $\tilde{d}_{1 \times 23 \times 4}$

$$\begin{aligned}
\tilde{d}_{1 \times 23 \times 4}(1^+, 2^+, 3^+, 4^+) &= C_{1 \times 2 \times 3 \times 4}^{(3)} \tilde{e}_{\{1^+ \times 2^+ \times 3^+ \times 4^+\}} \\
&\quad + \frac{2m^2}{\langle 12 \rangle \langle 23 \rangle \langle 34 \rangle \langle 41 \rangle} [(s_{12} + s_{13})(s_{24} + s_{34}) - s_{14}s_{23}]. \tag{4.4}
\end{aligned}$$

Coefficient	Related coefficients	Coefficient	Related coefficients
$\tilde{d}_{1 \times 2 \times 34}$	$\tilde{d}_{2 \times 3 \times 41}, \tilde{d}_{3 \times 4 \times 12}, \tilde{d}_{4 \times 1 \times 23},$ $\tilde{d}_{1 \times 4 \times 32}, \tilde{d}_{2 \times 1 \times 43}, \tilde{d}_{3 \times 2 \times 14}, \tilde{d}_{4 \times 3 \times 21}$	$\tilde{c}_{1 \times 234}$	$\tilde{c}_{2 \times 341}, \tilde{c}_{3 \times 412}, \tilde{c}_{4 \times 123}$
$\tilde{d}_{1 \times 23 \times 4}$	$\tilde{d}_{2 \times 34 \times 1}, \tilde{d}_{3 \times 41 \times 2}, \tilde{d}_{4 \times 12 \times 3}$		
$\tilde{d}_{1 \times 2 \times 3}$	$\tilde{d}_{2 \times 3 \times 4}, \tilde{d}_{3 \times 4 \times 1}, \tilde{d}_{4 \times 1 \times 2}$		

**Table 1.** Minimal set of integral coefficients for  $A_4^{1234}(g^+, g^+, g^+, g^+; h)$ .

#### 4.1.3 $\tilde{d}_{1 \times 2 \times 3}$

$$\begin{aligned} \tilde{d}_{1 \times 2 \times 3} &= \mathcal{C}_{4 \times 1 \times 2 \times 3}^{(1)} \tilde{e}_{\{4^+ \times 1^+ \times 2^+ \times 3^+\}} + \mathcal{C}_{1 \times 2 \times 3 \times 4}^{(5)} \tilde{e}_{\{1^+ \times 2^+ \times 3^+ \times 4^+\}} \\ &+ \frac{2m^2}{\langle 12 \rangle \langle 23 \rangle \langle 34 \rangle \langle 41 \rangle} s_{12} s_{23}. \end{aligned} \quad (4.5)$$

#### 4.1.4 $\tilde{c}_{1 \times 234}^{(0)}, \tilde{c}_{1 \times 234}^{(2)}$

$$\tilde{c}_{1 \times 234}^{(0)}(1^+, 2^+, 3^+, 4^+) = 0. \quad (4.6)$$

We have  $\tilde{c}_{1 \times 234}^{(2)}(1^+, 2^+, 3^+, 4^+) = c_{1 \times 234}^{(2)}(1^+, 2^+, 3^+, 4^+)$  where the fermionic coefficient is given in Eq. (4.10) of ref. [13].

#### 4.2 Coefficients for $A_4^{1234}(g^+, g^+, g^+, g^-; h)$

The effective pentagon coefficients [13] used to define the box coefficients below are,

$$\tilde{e}_{\{1^+ \times 2^+ \times 3^+ \times 4^-\}} = -4m^4 \frac{[23] \langle 4|(2+3)|1]}{\langle 23 \rangle \langle 1|(2+3)|4]}, \quad (4.7)$$

$$\tilde{e}_{\{4^- \times 1^+ \times 2^+ \times 3^+\}} = \tilde{e}_{\{1^+ \times 2^+ \times 3^+ \times 4^-\}} \{1 \leftrightarrow 3\}, \quad (4.8)$$

$$\tilde{e}_{\{2^+ \times 3^+ \times 4^- \times 1^+\}} = -4m^4 \frac{[23]^2 \langle 34 \rangle \langle 2|(3+4)|1]}{\langle 23 \rangle^2 [34] \langle 1|(3+4)|2]}, \quad (4.9)$$

$$\tilde{e}_{\{3^+ \times 4^- \times 1^+ \times 2^+\}} = \tilde{e}_{\{2^+ \times 3^+ \times 4^- \times 1^+\}} \{1 \leftrightarrow 3\}. \quad (4.10)$$

The minimal set of integral coefficients needed to reconstruct the amplitude for this approach is given in the first and third columns of Table 2.

#### 4.2.1 $\tilde{d}_{1 \times 2 \times 34}$

$$\begin{aligned} \tilde{d}_{1 \times 2 \times 34}(1^+, 2^+, 3^+, 4^-) &= \mathcal{C}_{1 \times 2 \times 3 \times 4}^{(4)} \tilde{e}_{\{1^+ \times 2^+ \times 3^+ \times 4^-\}} - 2m^2 \frac{[12]}{\langle 12 \rangle} \left[ \frac{\langle 24 \rangle^2 \langle 4|(2+3)|1]}{\langle 23 \rangle \langle 34 \rangle \langle 2|(3+4)|1]} \right. \\ &\left. + \frac{[23] \langle 1|(2+4)|3\rangle^2}{[34] \langle 1|(3+4)|2 \rangle \langle 1|(2+3)|4 \rangle} \right]. \end{aligned} \quad (4.11)$$

#### 4.2.2 $\tilde{d}_{1 \times 4 \times 32}$

$$\tilde{d}_{1 \times 4 \times 32}(1^+, 2^+, 3^+, 4^-) = \mathcal{C}_{2 \times 3 \times 4 \times 1}^{(2)} \tilde{e}_{\{2^+ \times 3^+ \times 4^- \times 1^+\}} + 2m^2 \frac{[23] s_{14} s_{234}^2}{\langle 23 \rangle^2 [34] \langle 1|(3+4)|2 \rangle \langle 1|(2+3)|4 \rangle}. \quad (4.12)$$

Coefficient	Related coefficients	Coefficient	Related coefficients
$\tilde{d}_{1 \times 2 \times 34}$	$\tilde{d}_{3 \times 2 \times 14}$	$\tilde{c}_{3 \times 4}$ (5.19)	$\tilde{c}_{4 \times 1}$
$\tilde{d}_{1 \times 4 \times 32}$	$\tilde{d}_{3 \times 4 \times 12}$	$\tilde{c}_{2 \times 34}$ (5.20)	$\tilde{c}_{2 \times 14}$
$\tilde{d}_{2 \times 1 \times 43}$	$\tilde{d}_{2 \times 3 \times 41}$	$\tilde{c}_{1 \times 43}$ (5.21)	$\tilde{c}_{3 \times 41}$
$\tilde{d}_{4 \times 3 \times 21}$	$\tilde{d}_{4 \times 1 \times 23}$	$\tilde{c}_{4 \times 123}$	
$\tilde{d}_{2 \times 34 \times 1}$	$\tilde{d}_{3 \times 41 \times 2}$	$\tilde{c}_{1 \times 234}$	$\tilde{c}_{3 \times 412}$
$\tilde{d}_{1 \times 23 \times 4}$	$\tilde{d}_{4 \times 12 \times 3}$	$\tilde{c}_{2 \times 341}$	
$\tilde{d}_{2 \times 3 \times 4}$	$\tilde{d}_{4 \times 1 \times 2}$	$\tilde{c}_{12 \times 34}$	$\tilde{c}_{23 \times 41}$
$\tilde{d}_{1 \times 2 \times 3}$		$\tilde{b}_{34}$ (5.30)	$\tilde{b}_{14}$
$\tilde{d}_{3 \times 4 \times 1}$		$\tilde{b}_{234}$ (5.31)	$\tilde{b}_{412}, \tilde{b}_{341}$
		$\tilde{b}_{1234}$ (5.32)	

**Table 2.** Minimal set of integral coefficients for  $A_4^{1234}(g^+, g^+, g^+, g^-; h)$ . The equation numbers in brackets give the place in ref. [13] where the coefficients are reported. These coefficients are the same in the scalar-mediated and the fermion-mediated theories.

#### 4.2.3 $\tilde{d}_{2 \times 1 \times 43}$

$$\begin{aligned} \tilde{d}_{2 \times 1 \times 43}(1^+, 2^+, 3^+, 4^-) &= C_{3 \times 4 \times 1 \times 2}^{(2)} \tilde{e}_{\{3^+ \times 4^- \times 1^+ \times 2^+\}} + 2m^2 \frac{[12]}{\langle 12 \rangle} \left[ \frac{[13]^2 \langle 2|(1+4)|3 \rangle}{[14] [34] \langle 2|(3+4)|1 \rangle} \right. \\ &\quad \left. + \frac{\langle 14 \rangle \langle 4|(1+3)|2 \rangle^2}{\langle 34 \rangle \langle 1|(3+4)|2 \rangle \langle 3|(1+4)|2 \rangle} \right]. \end{aligned} \quad (4.13)$$

#### 4.2.4 $\tilde{d}_{4 \times 3 \times 21}$

$$\tilde{d}_{4 \times 3 \times 21}(1^+, 2^+, 3^+, 4^-) = C_{1 \times 2 \times 3 \times 4}^{(2)} \tilde{e}_{\{1^+ \times 2^+ \times 3^+ \times 4^-\}} + 2m^2 \frac{s_{34} s_{123}^2}{\langle 12 \rangle \langle 23 \rangle \langle 1|(2+3)|4 \rangle \langle 3|(1+2)|4 \rangle}. \quad (4.14)$$

#### 4.2.5 $\tilde{d}_{1 \times 23 \times 4}$

$$\tilde{d}_{1 \times 23 \times 4}(1^+, 2^+, 3^+, 4^-) = C_{1 \times 2 \times 3 \times 4}^{(3)} \tilde{e}_{\{1^+ \times 2^+ \times 3^+ \times 4^-\}}. \quad (4.15)$$

#### 4.2.6 $\tilde{d}_{2 \times 34 \times 1}$

$$\begin{aligned} \tilde{d}_{2 \times 34 \times 1}(1^+, 2^+, 3^+, 4^-) &= C_{2 \times 3 \times 4 \times 1}^{(3)} \tilde{e}_{\{2^+ \times 3^+ \times 4^- \times 1^+\}} \\ &\quad + \frac{2 \langle 24 \rangle}{\langle 12 \rangle \langle 23 \rangle} \left[ \frac{\langle 14 \rangle \langle 24 \rangle \langle 1|(3+4)|2 \rangle \langle 2|(3+4)|1 \rangle}{\langle 12 \rangle^2 \langle 34 \rangle} \right. \\ &\quad \left. - m^2 \left( 3 \frac{\langle 14 \rangle \langle 24 \rangle [12]}{\langle 12 \rangle \langle 34 \rangle} + 2 \frac{[13] [23]}{[34]} + \frac{\langle 24 \rangle [14] [23]}{\langle 23 \rangle [34]} \right) \right]. \end{aligned} \quad (4.16)$$

#### 4.2.7 $\tilde{d}_{2 \times 3 \times 4}$

$$\begin{aligned} \tilde{d}_{2 \times 3 \times 4}(1^+, 2^+, 3^+, 4^-) &= C_{1 \times 2 \times 3 \times 4}^{(1)} \tilde{e}_{\{1^+ \times 2^+ \times 3^+ \times 4^-\}} + C_{2 \times 3 \times 4 \times 1}^{(5)} \tilde{e}_{\{2^+ \times 3^+ \times 4^- \times 1^+\}} \\ &\quad + 2m^2 \frac{s_{234} \langle 34 \rangle [23]^2}{\langle 23 \rangle \langle 1|(3+4)|2 \rangle \langle 1|(2+3)|4 \rangle}. \end{aligned} \quad (4.17)$$

#### 4.2.8 $\tilde{d}_{1 \times 2 \times 3}$

$$\begin{aligned} \tilde{d}_{1 \times 2 \times 3}(1^+, 2^+, 3^+, 4^-) &= C_{1 \times 2 \times 3 \times 4}^{(5)} \tilde{e}_{\{1^+ \times 2^+ \times 3^+ \times 4^-\}} + C_{4 \times 1 \times 2 \times 3}^{(1)} \tilde{e}_{\{4^- \times 1^+ \times 2^+ \times 3^+\}} \\ &+ 2m^2 \frac{s_{123} [12] [23]}{\langle 3|(1+2)|4\rangle \langle 1|(2+3)|4\rangle}. \end{aligned} \quad (4.18)$$

#### 4.2.9 $\tilde{d}_{3 \times 4 \times 1}$

$$\begin{aligned} \tilde{d}_{3 \times 4 \times 1}(1^+, 2^+, 3^+, 4^-) &= C_{2 \times 3 \times 4 \times 1}^{(1)} \tilde{e}_{\{2^+ \times 3^+ \times 4^- \times 1^+\}} + C_{3 \times 4 \times 1 \times 2}^{(5)} \tilde{e}_{\{3^+ \times 4^- \times 1^+ \times 2^+\}} \\ &- 2m^2 \frac{1}{\langle 13\rangle} \left[ \frac{[23] \langle 34\rangle^2 s_{14}}{\langle 23\rangle^2 \langle 1|(3+4)|2\rangle} + \frac{[12] \langle 14\rangle^2 s_{34}}{\langle 12\rangle^2 \langle 3|(1+4)|2\rangle} \right] \\ &+ \frac{\langle 14\rangle \langle 34\rangle}{\langle 12\rangle \langle 13\rangle^2 \langle 23\rangle} \left[ 2s_{14} s_{34} + 6m^2 s_{13} \right]. \end{aligned} \quad (4.19)$$

#### 4.2.10 $\tilde{c}_{4 \times 123}^{(0)}, \tilde{c}_{4 \times 123}^{(2)}$

$$\tilde{c}_{4 \times 123}^{(0)}(1^+, 2^+, 3^+, 4^-) = 0. \quad (4.20)$$

We have  $\tilde{c}_{4 \times 123}^{(2)}(1^+, 2^+, 3^+, 4^-) = c_{4 \times 123}^{(2)}(1^+, 2^+, 3^+, 4^-)$ , where the fermionic coefficient is given in Eq. (5.23) of ref. [13].

#### 4.2.11 $\tilde{c}_{1 \times 234}^{(0)}, \tilde{c}_{1 \times 234}^{(2)}$

$$\tilde{c}_{1 \times 234}^{(0)}(1^+, 2^+, 3^+, 4^-) = 2(s_{12} + s_{13} + s_{14}) \frac{\langle 14\rangle \langle 24\rangle^2}{\langle 12\rangle^3 \langle 23\rangle \langle 34\rangle}. \quad (4.21)$$

Also, we have  $\tilde{c}_{1 \times 234}^{(2)}(1^+, 2^+, 3^+, 4^-) = c_{1 \times 234}^{(2)}(1^+, 2^+, 3^+, 4^-)$ , where the fermionic coefficient is given in Eq. (5.25) of ref. [13].

#### 4.2.12 $\tilde{c}_{2 \times 341}^{(0)}, \tilde{c}_{2 \times 341}^{(2)}$

$$\tilde{c}_{2 \times 341}^{(0)}(1^+, 2^+, 3^+, 4^-) = 2(s_{12} + s_{23} + s_{24}) \langle 24\rangle^2 \frac{\langle 14\rangle^2 \langle 23\rangle^2 + \langle 12\rangle^2 \langle 34\rangle^2}{\langle 12\rangle^3 \langle 23\rangle^3 \langle 14\rangle \langle 34\rangle}. \quad (4.22)$$

Furthermore,  $\tilde{c}_{2 \times 341}^{(2)}(1^+, 2^+, 3^+, 4^-) = c_{2 \times 341}^{(2)}(1^+, 2^+, 3^+, 4^-)$ , where the fermionic coefficient is given in Eq. (5.27) of ref. [13].

#### 4.2.13 $\tilde{c}_{12 \times 34}^{(0)}, \tilde{c}_{12 \times 34}^{(2)}$

$$\tilde{c}_{12 \times 34}^{(0)}(1^+, 2^+, 3^+, 4^-) = 0. \quad (4.23)$$

In addition,  $\tilde{c}_{12 \times 34}^{(2)}(1^+, 2^+, 3^+, 4^-) = c_{12 \times 34}^{(2)}(1^+, 2^+, 3^+, 4^-)$ , where the fermionic coefficient is given in Eq. (5.29) of ref. [13].

Coefficient	Related coefficients	Coefficient	Related coefficients
$\tilde{d}_{4 \times 3 \times 21}$	$\tilde{d}_{2 \times 1 \times 43}, \tilde{d}_{3 \times 2 \times 14}, \tilde{d}_{1 \times 4 \times 32},$ $\tilde{d}_{1 \times 2 \times 34}, \tilde{d}_{2 \times 3 \times 41},$ $\tilde{d}_{3 \times 4 \times 12}, \tilde{d}_{4 \times 1 \times 23}$	$\tilde{c}_{3 \times 4}$ (6.9) $\tilde{c}_{2 \times 34}$ (6.10)	$\tilde{c}_{4 \times 1}, \tilde{c}_{2 \times 3}, \tilde{c}_{1 \times 2}$ $\tilde{c}_{3 \times 41}, \tilde{c}_{4 \times 12}, \tilde{c}_{1 \times 23}$ $\tilde{c}_{1 \times 43}, \tilde{c}_{2 \times 14}, \tilde{c}_{3 \times 21}, \tilde{c}_{4 \times 32}$
$\tilde{d}_{1 \times 23 \times 4}$	$\tilde{d}_{2 \times 34 \times 1}, \tilde{d}_{3 \times 41 \times 2}, \tilde{d}_{4 \times 12 \times 3}$	$\tilde{c}_{12 \times 34}$	$\tilde{c}_{23 \times 41}$
$\tilde{d}_{1 \times 2 \times 3}$	$\tilde{d}_{2 \times 3 \times 4}, \tilde{d}_{3 \times 4 \times 1}, \tilde{d}_{4 \times 1 \times 2}$	$\tilde{c}_{1 \times 234}$ $\tilde{b}_{34}$ (6.17) $\tilde{b}_{234}$ (6.18) $\tilde{b}_{1234}$ (6.19)	$\tilde{c}_{2 \times 341}, \tilde{c}_{3 \times 412}, \tilde{c}_{4 \times 123}$ $\tilde{b}_{12}, \tilde{b}_{23}, \tilde{b}_{41}$ $\tilde{b}_{341}, \tilde{b}_{412}, \tilde{b}_{123}$

**Table 3.** Minimal set of integral coefficients for  $A_4^{1234}(g^+, g^-, g^+, g^-; h)$ . The equation numbers in brackets give the place in ref. [13] where the coefficients are reported. These coefficients are the same in the scalar-mediated and the fermion-mediated theories.

### 4.3 Coefficients for $A_4^{1234}(g^+, g^-, g^+, g^-; h)$

The effective pentagon coefficients for this helicity combination are,

$$\tilde{e}_{\{1^+ \times 2^- \times 3^+ \times 4^-\}} = -4m^4 \frac{\langle 12 \rangle [34] \langle 4|(2+3)|1 \rangle^2}{[12] \langle 34 \rangle \langle 1|(2+3)|4 \rangle^2}, \quad (4.24)$$

$$\tilde{e}_{\{3^+ \times 4^- \times 1^+ \times 2^-\}} = \tilde{e}_{\{1^+ \times 2^- \times 3^+ \times 4^-\}} \left\{ 1 \leftrightarrow 3, 2 \leftrightarrow 4 \right\}, \quad (4.25)$$

$$\tilde{e}_{\{4^- \times 1^+ \times 2^- \times 3^+\}} = \tilde{e}_{\{1^+ \times 2^- \times 3^+ \times 4^-\}} \left\{ 1 \rightarrow 4, 2 \rightarrow 1, 3 \rightarrow 2, 4 \rightarrow 3, \langle \rangle \leftrightarrow [] \right\}, \quad (4.26)$$

$$\tilde{e}_{\{2^- \times 3^+ \times 4^- \times 1^+\}} = \tilde{e}_{\{1^+ \times 2^- \times 3^+ \times 4^-\}} \left\{ 1 \rightarrow 2, 2 \rightarrow 3, 3 \rightarrow 4, 4 \rightarrow 1, \langle \rangle \leftrightarrow [] \right\}. \quad (4.27)$$

The minimal set of coefficients that needs to be calculated is given in Table 3.

#### 4.3.1 $\tilde{d}_{4 \times 3 \times 21}$

$$\begin{aligned} \tilde{d}_{4 \times 3 \times 21}(1^+, 2^-, 3^+, 4^-) &= \tilde{e}_{\{1^+ \times 2^- \times 3^+ \times 4^-\}} \mathcal{C}_{1 \times 2 \times 3 \times 4}^{(2)} \\ &\quad - \frac{2 \langle 2|(1+3)|4 \rangle}{\langle 1|(2+3)|4 \rangle \langle 3|(1+2)|4 \rangle} \left[ \frac{\langle 23 \rangle \langle 2|(1+3)|4 \rangle s_{34} s_{123}^2}{\langle 12 \rangle \langle 3|(1+2)|4 \rangle^2} \right. \\ &\quad + m^2 \left( 2 \frac{[13] \langle 4|(2+3)|1 \rangle}{[12]} + \frac{[23] \langle 2|(1+3)|4 \rangle \langle 4|(2+3)|1 \rangle}{[12] \langle 1|(2+3)|4 \rangle} \right. \\ &\quad \left. \left. + 3 \frac{\langle 23 \rangle \langle 2|(1+3)|4 \rangle \langle 4|(1+2)|3 \rangle}{\langle 12 \rangle \langle 3|(1+2)|4 \rangle} \right) \right]. \end{aligned} \quad (4.28)$$

#### 4.3.2 $\tilde{d}_{1 \times 23 \times 4}$

$$\begin{aligned} \tilde{d}_{1 \times 23 \times 4}(1^+, 2^-, 3^+, 4^-) &= \tilde{e}_{\{1^+ \times 2^- \times 3^+ \times 4^-\}} \mathcal{C}_{1 \times 2 \times 3 \times 4}^{(3)} \\ &\quad - 2m^2 \frac{\langle 4|(2+3)|1 \rangle}{\langle 1|(2+3)|4 \rangle} \left[ \frac{\langle 12 \rangle \langle 24 \rangle^2}{\langle 14 \rangle \langle 23 \rangle \langle 34 \rangle} + \frac{[13]^2 [34]}{[12] [14] [23]} \right]. \end{aligned} \quad (4.29)$$

### 4.3.3 $\tilde{d}_{1 \times 2 \times 3}$

$$\begin{aligned}
\tilde{d}_{1 \times 2 \times 3}(1^+, 2^-, 3^+, 4^-) &= \mathcal{C}_{1 \times 2 \times 3 \times 4}^{(5)} \tilde{e}_{\{1^+ \times 2^- \times 3^+ \times 4^-\}} + \mathcal{C}_{4 \times 1 \times 2 \times 3}^{(1)} \tilde{e}_{\{4^- \times 1^+ \times 2^- \times 3^+\}} \\
&+ \frac{\langle 12 \rangle \langle 23 \rangle}{\langle 1|(2+3)|4 \rangle \langle 3|(1+2)|4 \rangle} \left[ -2 \frac{s_{12} s_{23} s_{123}}{\langle 13 \rangle^2} + 2m^2 \left( 2 \frac{[13] s_{123}}{\langle 13 \rangle} \right. \right. \\
&- [13]^2 + \frac{[12][23]\langle 24 \rangle^2}{\langle 14 \rangle \langle 34 \rangle} - \frac{[23]\langle 2|(1+3)|4 \rangle \langle 4|(2+3)|1 \rangle}{\langle 34 \rangle \langle 1|(2+3)|4 \rangle} \\
&\left. \left. + \frac{[12]\langle 2|(1+3)|4 \rangle \langle 4|(1+2)|3 \rangle}{\langle 14 \rangle \langle 3|(1+2)|4 \rangle} \right) \right]. \tag{4.30}
\end{aligned}$$

### 4.3.4 $\tilde{c}_{12 \times 34}^{(0)}, \tilde{c}_{12 \times 34}^{(2)}$

In this case the scalar coefficient  $\tilde{c}_{12 \times 34}^{(0)}(1^+, 2^-, 3^+, 4^-)$  has been given previously, in Eq. (6.13) of Ref. [13]. Moreover,  $\tilde{c}_{12 \times 34}^{(2)}(1^+, 2^-, 3^+, 4^-) = c_{12 \times 34}^{(2)}(1^+, 2^-, 3^+, 4^-)$ , where the fermionic coefficient is given in Eq. (6.12) of ref. [13].

### 4.3.5 $\tilde{c}_{1 \times 234}^{(0)}, \tilde{c}_{1 \times 234}^{(2)}$

$$\begin{aligned}
\tilde{c}_{1 \times 234}^{(0)}(1^+, 2^-, 3^+, 4^-) &= -2(s_{12} + s_{13} + s_{14}) \frac{s_{234} \langle 1|(2+4)|3 \rangle^2}{[23][34] \langle 1|(2+3)|4 \rangle^3 \langle 1|(3+4)|2 \rangle^3} \\
&\times \left( [23]^2 \langle 1|(2+3)|4 \rangle^2 + [34]^2 \langle 1|(3+4)|2 \rangle^2 \right). \tag{4.31}
\end{aligned}$$

In addition, we have  $\tilde{c}_{1 \times 234}^{(2)}(1^+, 2^-, 3^+, 4^-) = c_{1 \times 234}^{(2)}(1^+, 2^-, 3^+, 4^-)$ , where the fermionic coefficient is given in Eq. (6.16) of ref. [13].

## 4.4 Coefficients for $A_4^{1234}(g^+, g^+, g^-, g^-; h)$

The effective pentagon coefficients are given by,

$$\tilde{e}_{\{1^+ \times 2^+ \times 3^- \times 4^-\}} = -4m^4 \frac{[12]\langle 34 \rangle}{\langle 12 \rangle [34]}, \tag{4.32}$$

$$\tilde{e}_{\{2^+ \times 3^- \times 4^- \times 1^+\}} = -4m^4 \frac{[23]\langle 34 \rangle^2 [41]}{\langle 23 \rangle [34]^2 \langle 41 \rangle}, \tag{4.33}$$

$$\tilde{e}_{\{2^+ \times 3^- \times 4^- \times 1^+\}} = -4m^4 \frac{[23]\langle 34 \rangle^2 [41]}{\langle 23 \rangle [34]^2 \langle 41 \rangle}, \tag{4.34}$$

$$\tilde{e}_{\{4^- \times 1^+ \times 2^+ \times 3^-\}} = \tilde{e}_{\{2^+ \times 3^- \times 4^- \times 1^+\}} \{2 \leftrightarrow 4, 1 \leftrightarrow 3, \langle \rangle \leftrightarrow [\ ]\}. \tag{4.35}$$

The minimal set of coefficients that needs to be calculated is given in Table 4.

### 4.4.1 $\tilde{d}_{1 \times 2 \times 34}$

$$\tilde{d}_{1 \times 2 \times 34}(1^+, 2^+, 3^-, 4^-) = \mathcal{C}_{1 \times 2 \times 3 \times 4}^{(4)} \tilde{e}_{\{1^+ \times 2^+ \times 3^- \times 4^-\}}. \tag{4.36}$$

Coefficient	Related coefficients	Coefficient	Related coefficients
$\tilde{d}_{1 \times 2 \times 34}$	$\tilde{d}_{2 \times 1 \times 43}, \tilde{d}_{3 \times 4 \times 12}, \tilde{d}_{4 \times 3 \times 21}$	$\tilde{c}_{2 \times 3}$ (7.10)	$\tilde{c}_{4 \times 1}$
$\tilde{d}_{1 \times 4 \times 32}$	$\tilde{d}_{3 \times 2 \times 14}, \tilde{d}_{4 \times 1 \times 23}, \tilde{d}_{2 \times 3 \times 41}$	$\tilde{c}_{1 \times 23}$ (7.11)	$\tilde{c}_{2 \times 14}, \tilde{c}_{3 \times 41}, \tilde{c}_{4 \times 32}$
$\tilde{d}_{2 \times 34 \times 1}$	$\tilde{d}_{4 \times 12 \times 3}$	$\tilde{c}_{1 \times 234}$	$\tilde{c}_{2 \times 341}, \tilde{c}_{3 \times 412}, \tilde{c}_{4 \times 123}$
$\tilde{d}_{1 \times 23 \times 4}$	$\tilde{d}_{3 \times 41 \times 2}$	$\tilde{c}_{23 \times 41}$	
$\tilde{d}_{1 \times 2 \times 3}$	$\tilde{d}_{3 \times 4 \times 1}, \tilde{d}_{4 \times 1 \times 2}, \tilde{d}_{2 \times 3 \times 4}$	$\tilde{b}_{23}$ (7.17)	$\tilde{b}_{41}$
		$\tilde{b}_{234}$ (7.18)	$\tilde{b}_{341}, \tilde{b}_{412}, \tilde{b}_{123}$
		$\tilde{b}_{1234}$ (7.19)	

**Table 4.** Minimal set of integral coefficients for  $A_4^{1234}(g^+, g^+, g^-, g^-; h)$ . The equation numbers in brackets give the place in ref. [13] where the coefficients are reported. These coefficients are the same in the scalar-mediated and the fermion-mediated theories.

#### 4.4.2 $\tilde{d}_{1 \times 4 \times 32}$

$$\begin{aligned} \tilde{d}_{1 \times 4 \times 32}(1^+, 2^+, 3^-, 4^-) &= \mathcal{C}_{2 \times 3 \times 4 \times 1}^{(2)} \tilde{e}_{\{2^+ \times 3^- \times 4^- \times 1^+\}} - 2 \frac{[24]^2}{\langle 1|(2+3)|4\rangle [34]} \left\{ \frac{s_{14} s_{234}^2 \langle 1|(3+4)|2\rangle}{[23] \langle 1|(2+3)|4\rangle^2} \right. \\ &\quad \left. + m^2 \left[ 3 \frac{\langle 1|(3+4)|2\rangle \langle 4|(2+3)|1\rangle}{[23] \langle 1|(2+3)|4\rangle} + \frac{[14] \langle 34\rangle s_{234}}{\langle 23\rangle [24] [34]} + \frac{\langle 34\rangle \langle 3|(2+4)|1\rangle}{\langle 23\rangle [24]} \right] \right\}. \end{aligned} \quad (4.37)$$

#### 4.4.3 $\tilde{d}_{2 \times 34 \times 1}$

$$\tilde{d}_{2 \times 34 \times 1}(1^+, 2^+, 3^-, 4^-) = \mathcal{C}_{2 \times 3 \times 4 \times 1}^{(3)} \tilde{e}_{\{2^+ \times 3^- \times 4^- \times 1^+\}} - 2m^2 \frac{\langle 34\rangle \langle 1|(3+4)|2\rangle \langle 2|(3+4)|1\rangle}{\langle 12\rangle \langle 14\rangle \langle 23\rangle [34]^2}. \quad (4.38)$$

#### 4.4.4 $\tilde{d}_{1 \times 23 \times 4}$

$$\begin{aligned} \tilde{d}_{1 \times 23 \times 4}(1^+, 2^+, 3^-, 4^-) &= \mathcal{C}_{1 \times 2 \times 3 \times 4}^{(3)} \tilde{e}_{\{1^+ \times 2^+ \times 3^- \times 4^-\}} \\ &\quad + 2m^2 \frac{\langle 4|(2+3)|1\rangle}{\langle 12\rangle [34] \langle 1|(2+3)|4\rangle} \times \left[ \frac{s_{12} [24]^2}{[14] [23]} + \frac{s_{34} \langle 13\rangle^2}{\langle 23\rangle \langle 14\rangle} \right]. \end{aligned} \quad (4.39)$$

#### 4.4.5 $\tilde{d}_{1 \times 2 \times 3}$

$$\begin{aligned} \tilde{d}_{1 \times 2 \times 3}(1^+, 2^+, 3^-, 4^-) &= \mathcal{C}_{1 \times 2 \times 3 \times 4}^{(5)} \tilde{e}_{\{1^+ \times 2^+ \times 3^- \times 4^-\}} + \mathcal{C}_{4 \times 1 \times 2 \times 3}^{(1)} \tilde{e}_{\{4^- \times 1^+ \times 2^+ \times 3^-\}} \\ &\quad - 2m^2 \frac{[12]^2 \langle 23\rangle}{\langle 12\rangle [14] [34]}. \end{aligned} \quad (4.40)$$

#### 4.4.6 $\tilde{c}_{23 \times 41}^{(0)}, \tilde{c}_{23 \times 41}^{(2)}$

$$\begin{aligned} \tilde{c}_{23 \times 41}^{(0)}(1^+, 2^+, 3^-, 4^-) &= -\tilde{c}_{12 \times 34}^{(0)}(2^+, 3^-, 1^+, 4^-) - \left\{ 2 \Delta_3(1, 4, 2, 3) \left[ \frac{(s_{13} - s_{24})}{\langle 2|(1+4)|3\rangle \langle 1|(2+3)|4\rangle} \right]^2 \right. \\ &\quad \left. + 4 \frac{\langle 3|(1+4)|2\rangle \langle 4|(2+3)|1\rangle}{\langle 2|(1+4)|3\rangle \langle 1|(2+3)|4\rangle} \right\}. \end{aligned} \quad (4.41)$$

$1_q^+, 2_q^-, 3_g^+, 4_g^+$		$1_q^+, 2_q^-, 3_g^-, 4_g^+$		$1_q^+, 2_q^-, 3_g^+, 4_g^-$
Coefficient	Related coefficient	Coefficient	Related coefficient	Coefficient
$\tilde{d}_{3 \times 21 \times 4}$		$\tilde{d}_{3 \times 21 \times 4}$		$\tilde{c}_{4 \times 123}$
$\tilde{d}_{4 \times 3 \times 21}$	$\tilde{d}_{3 \times 4 \times 12}$	$\tilde{d}_{4 \times 3 \times 21}$	$\tilde{d}_{3 \times 4 \times 12}$	$\tilde{b}_{123}$ (10.4)
$\tilde{c}_{3 \times 21}$ (8.4)	$\tilde{c}_{4 \times 12}$	$\tilde{c}_{3 \times 4}$ (9.3)		
$\tilde{c}_{12 \times 34}$		$\tilde{c}_{3 \times 21}$ (9.4)	$\tilde{c}_{4 \times 12}$	
$\tilde{c}_{4 \times 123}$		$\tilde{c}_{12 \times 34}$		
$\tilde{c}_{3 \times 412}$		$\tilde{c}_{4 \times 123}$	$\tilde{c}_{3 \times 412}$	
$\tilde{b}_{12}$ (8.11)		$\tilde{b}_{34}$ (9.9)		
$\tilde{b}_{123}$ (8.12)		$\tilde{b}_{12}$ (9.10)		
$\tilde{b}_{412}$ (8.13)		$\tilde{b}_{123}$ (9.11)	$\tilde{b}_{412}$	
$\tilde{b}_{1234}$ (8.14)		$\tilde{b}_{1234}$ (9.12)		

**Table 5.** Minimal set of integral coefficients for  $A_4^{34}(1_q^+, 2_q^-, 3_g^+, 4_g^+)$ ,  $A_4^{34}(1_q^+, 2_q^-, 3_g^-, 4_g^+)$  and  $A_4^{34}(1_q^+, 2_q^-, 3_g^+, 4_g^-)$  together with the related coefficients that can be obtained from the base set. The equation numbers in brackets give the place in ref. [13] where the coefficients are reported. These coefficients are the same in the scalar-mediated and the fermion-mediated theories.

Moreover,  $\tilde{c}_{23 \times 41}^{(2)}(1^+, 2^+, 3^-, 4^-) = c_{23 \times 41}^{(2)}(1^+, 2^+, 3^-, 4^-)$ , where the fermionic coefficient is given in Eq. (7.14) of ref. [13].

#### 4.4.7 $\tilde{c}_{1 \times 234}^{(0)}, \tilde{c}_{1 \times 234}^{(2)}$

$$\tilde{c}_{1 \times 234}^{(0)}(1^+, 2^+, 3^-, 4^-) = -2(s_{12} + s_{13} + s_{14}) s_{234} \frac{\langle 1|(3+4)|2\rangle [24]^2}{\langle 1|(2+3)|4\rangle^3 [23][34]}. \quad (4.42)$$

Furthermore,  $\tilde{c}_{1 \times 234}^{(2)}(1^+, 2^+, 3^-, 4^-) = c_{1 \times 234}^{(2)}(1^+, 2^+, 3^-, 4^-)$ , where the fermionic coefficient is given in Eq. (7.16) of ref. [13].

#### 4.5 Coefficients for $A_4^{34}(\bar{q}^+, q^-, g^+, g^+; h)$

The coefficients that must be computed for this amplitude are shown in the left-hand column of Table 5.

##### 4.5.1 $\tilde{d}_{3 \times 21 \times 4}$

$$\begin{aligned} \tilde{d}_{3 \times 21 \times 4}(1_q^+, 2_q^-, 3_g^+, 4_g^+) &= -2 \frac{\langle 24 \rangle \langle 23 \rangle}{\langle 12 \rangle \langle 34 \rangle^3} \left[ (s_{13} + s_{23})(s_{14} + s_{24}) - s_{12} s_{34} \right] \\ &\quad + 2m^2 \left[ \frac{[13][14]}{[12]\langle 34 \rangle} + 3 \frac{\langle 23 \rangle \langle 24 \rangle [34]}{\langle 12 \rangle \langle 34 \rangle^2} \right]. \end{aligned} \quad (4.43)$$

##### 4.5.2 $\tilde{d}_{4 \times 3 \times 21}$

$$\tilde{d}_{4 \times 3 \times 21}(1_q^+, 2_q^-, 3_g^+, 4_g^+) = 2m^2 \frac{[34]}{\langle 34 \rangle} \left[ \frac{\langle 23 \rangle \langle 2|(1+3)|4\rangle}{\langle 12 \rangle \langle 3|(1+2)|4\rangle} - \frac{[13] \langle 4|(2+3)|1\rangle}{[12] \langle 4|(1+2)|3\rangle} \right]. \quad (4.44)$$

**4.5.3**  $\tilde{c}_{12 \times 34}^{(0)}, \tilde{c}_{12 \times 34}^{(2)}$

$$\tilde{c}_{12 \times 34}^{(0)}(1_{\bar{q}}^+, 2_q^-, 3_g^+, 4_g^+) = 0. \quad (4.45)$$

The coefficient  $\tilde{c}_{12 \times 34}^{(2)}(1_{\bar{q}}^+, 2_q^-, 3_g^+, 4_g^+)$  is identical to  $c_{12 \times 34}^{(2)}(1_{\bar{q}}^+, 2_q^-, 3_g^+, 4_g^+)$  given in Eq. (8.6) of ref. [13].

**4.5.4**  $\tilde{c}_{4 \times 123}^{(0)}, \tilde{c}_{4 \times 123}^{(2)}$

$$\tilde{c}_{4 \times 123}^{(0)}(1_{\bar{q}}^+, 2_q^-, 3_g^+, 4_g^+) = -2(s_{14} + s_{24} + s_{34}) \left[ \frac{\langle 23 \rangle \langle 24 \rangle}{\langle 12 \rangle \langle 34 \rangle^3} \right]. \quad (4.46)$$

The coefficient  $\tilde{c}_{4 \times 123}^{(2)}(1_{\bar{q}}^+, 2_q^-, 3_g^+, 4_g^+)$  is identical to  $c_{4 \times 123}^{(2)}(1_{\bar{q}}^+, 2_q^-, 3_g^+, 4_g^+)$  given in Eq. (8.8) of ref. [13].

**4.5.5**  $\tilde{c}_{3 \times 412}^{(0)}, \tilde{c}_{3 \times 412}^{(2)}$

$$\tilde{c}_{3 \times 412}^{(0)}(1_{\bar{q}}^+, 2_q^-, 3_g^+, 4_g^+) = -2(s_{13} + s_{23} + s_{34}) \left[ \frac{\langle 23 \rangle \langle 24 \rangle}{\langle 12 \rangle \langle 34 \rangle^3} \right]. \quad (4.47)$$

The coefficient  $\tilde{c}_{3 \times 412}^{(2)}(1_{\bar{q}}^+, 2_q^-, 3_g^+, 4_g^+)$  is identical to  $c_{3 \times 412}^{(2)}(1_{\bar{q}}^+, 2_q^-, 3_g^+, 4_g^+)$  given in Eq. (8.10) of ref. [13].

**4.6 Coefficients for  $A_4^{34}(\bar{q}^+, q^-, g^-, g^+; h)$**

The coefficients that must be computed for this amplitude are shown in the middle column of Table 5.

**4.6.1**  $\tilde{d}_{3 \times 21 \times 4}$

$$\tilde{d}_{3 \times 21 \times 4}(1_{\bar{q}}^+, 2_q^-, 3_g^-, 4_g^+) = 2m^2 \frac{\langle 3|(1+2)|4 \rangle}{\langle 4|(1+2)|3 \rangle} \left[ \frac{\langle 23 \rangle \langle 24 \rangle}{\langle 12 \rangle \langle 34 \rangle} - \frac{[13][14]}{[12][34]} \right]. \quad (4.48)$$

**4.6.2**  $\tilde{d}_{4 \times 3 \times 21}$

$$\begin{aligned} \tilde{d}_{4 \times 3 \times 21}(1_{\bar{q}}^+, 2_q^-, 3_g^-, 4_g^+) = & \frac{-2}{\langle 4|(1+2)|3 \rangle} \left\{ \frac{[13] \langle 4|(2+3)|1 \rangle s_{34} s_{123}^2}{[12] \langle 4|(1+2)|3 \rangle^2} \right. \\ & \left. + m^2 \left[ \frac{3[13] \langle 3|(1+2)|4 \rangle \langle 4|(2+3)|1 \rangle}{[12] \langle 4|(1+2)|3 \rangle} + \frac{\langle 23 \rangle \langle 2|(1+3)|4 \rangle}{\langle 12 \rangle} \right] \right\}. \quad (4.49) \end{aligned}$$

### 4.6.3 $\tilde{c}_{12 \times 34}^{(0)}, \tilde{c}_{12 \times 34}^{(2)}$

$$\begin{aligned}
\tilde{c}_{12 \times 34}^{(0)}(1_{\bar{q}}^+, 2_q^-, 3_g^-, 4_g^+) &= 8(s_{124} - s_{123})(s_{12} + s_{34} + 2s_{13} + 2s_{23}) \frac{\langle 24 \rangle [13] \langle 3|(1+2)|4 \rangle}{\langle 4|(1+2)|3 \rangle^2 \Delta_3(1, 2, 3, 4)} \\
&+ \left( (9s_{13} - 7s_{23} - s_{14} - s_{24} + 4s_{34}) \langle 24 \rangle [14] \right. \\
&- \left. (9s_{14} - 7s_{24} - s_{13} - s_{23} + 4s_{34}) \langle 23 \rangle [13] \right) \times \frac{1}{\langle 4|(1+2)|3 \rangle^2} \\
&+ 12 \frac{s_{1234}((s_{13} + s_{23})^2 - (s_{14} + s_{24})^2) \langle 2|(3+4)|1 \rangle \langle 3|(1+2)|4 \rangle}{\langle 4|(1+2)|3 \rangle \Delta_3(1, 2, 3, 4)^2} \\
&+ 4 \left\{ 3(s_{12} + s_{34}) + 4(s_{13} + s_{23} + s_{14}) \right\} [13] \langle 23 \rangle \\
&- \left\{ 3(s_{12} + s_{34}) + 4(s_{13} + s_{24} + s_{14}) \right\} [14] \langle 24 \rangle \Big) \times \frac{\langle 3|(1+2)|4 \rangle}{\langle 4|(1+2)|3 \rangle \Delta_3(1, 2, 3, 4)} \\
&- 24 \frac{[13] \langle 24 \rangle \langle 3|(1+2)|4 \rangle^2}{\langle 4|(1+2)|3 \rangle \Delta_3(1, 2, 3, 4)} - 8 \frac{[14] \langle 23 \rangle \langle 3|(1+2)|4 \rangle}{\Delta_3(1, 2, 3, 4)} + 8 \frac{[14] \langle 23 \rangle}{\langle 4|(1+2)|3 \rangle} \\
&+ \left\{ \frac{2 \langle 24 \rangle^2 [34] (s_{14} + s_{24})^2}{\langle 12 \rangle \langle 4|(1+2)|3 \rangle^3} + \frac{[13] \langle 24 \rangle (s_{14} + s_{24}) (4s_{124} - 2s_{34})}{\langle 4|(1+2)|3 \rangle^3} \right. \\
&+ \left. \frac{2 \langle 23 \rangle \langle 24 \rangle [34] (s_{14} + s_{24})}{\langle 12 \rangle \langle 4|(1+2)|3 \rangle^2} - \frac{\langle 23 \rangle [13] (s_{14} + s_{24} - s_{13} - s_{23})}{\langle 4|(1+2)|3 \rangle^2} \right\} \\
&- \left\{ 1 \leftrightarrow 2, 3 \leftrightarrow 4, \langle \rangle \leftrightarrow [] \right\}. \tag{4.50}
\end{aligned}$$

The coefficient  $\tilde{c}_{12 \times 34}^{(2)}(1_{\bar{q}}^+, 2_q^-, 3_g^-, 4_g^+)$  is identical to  $c_{12 \times 34}^{(2)}(1_{\bar{q}}^+, 2_q^-, 3_g^-, 4_g^+)$  given in Eq. (9.6) of ref. [13].

### 4.6.4 $\tilde{c}_{4 \times 123}^{(0)}, \tilde{c}_{4 \times 123}^{(2)}$

$$\tilde{c}_{4 \times 123}^{(0)}(1_{\bar{q}}^+, 2_q^-, 3_g^-, 4_g^+) = - \frac{2(s_{14} + s_{24} + s_{34}) [13] \langle 4|(2+3)|1 \rangle s_{123}}{[12] \langle 4|(1+2)|3 \rangle^3}. \tag{4.51}$$

The coefficient  $\tilde{c}_{4 \times 123}^{(2)}(1_{\bar{q}}^+, 2_q^-, 3_g^-, 4_g^+)$  is identical to  $c_{4 \times 123}^{(2)}(1_{\bar{q}}^+, 2_q^-, 3_g^-, 4_g^+)$  given in Eq. (9.8) of ref. [13].

## 4.7 Coefficients for $A_4^{34}(\bar{q}^+, q^-, g^+, g^-; h)$

The coefficients for this amplitude that cannot be obtained from those for  $H_4^{34}(\bar{q}^+, q^-, g^-, g^+)$  by performing the following operation:  $1 \leftrightarrow 2, \langle \rangle \leftrightarrow []$ , are listed in the right-most column of Table 5. The explicit form of  $\tilde{c}_{4 \times 123}$  is given here, whereas  $b_{123}$  remains unaltered as compared to the fermion case.

### 4.7.1 $\tilde{c}_{4 \times 123}^{(0)}, \tilde{c}_{4 \times 123}^{(2)}$

$$\tilde{c}_{4 \times 123}^{(0)}(1_{\bar{q}}^+, 2_q^-, 3_g^+, 4_g^-) = \frac{2 \langle 2|(1+3)|4 \rangle s_{123}}{\langle 12 \rangle \langle 3|(1+2)|4 \rangle^2} \left\{ \langle 24 \rangle - \langle 34 \rangle \frac{\langle 2|(1+3)|4 \rangle}{\langle 3|(1+2)|4 \rangle} \right\}. \tag{4.52}$$

The coefficient  $\tilde{c}_{4 \times 123}^{(2)}(1_{\bar{q}}^+, 2_q^-, 3_g^+, 4_g^-)$  is identical to  $c_{4 \times 123}^{(2)}(1_{\bar{q}}^+, 2_q^-, 3_g^+, 4_g^-)$  given in Eq. (10.3) of ref. [13].

## 4.8 Amplitude for $0 \rightarrow \bar{q}q\bar{q}qh$

This calculation proceeds in a similar way to the calculation for a loop of fermions detailed in ref. [26]. The amplitude can be obtained by considering the tensor current for the scalar-mediated process  $0 \rightarrow ggh$ , with two off-shell gluons (with momenta  $k_1$  and  $k_2$ ),

$$\mathcal{T}^{\mu_1\mu_2}(k_1, k_2) = -i\delta^{c_1c_2} \frac{g_s^2}{8\pi^2} \left( \frac{-\lambda}{4} \right) \left[ \tilde{F}_T(k_1, k_2) T_T^{\mu_1\mu_2} + \tilde{F}_L(k_1, k_2) T_L^{\mu_1\mu_2} \right]. \quad (4.53)$$

The two tensor structures appearing here are,

$$T_T^{\mu_1\mu_2} = k_1 \cdot k_2 g^{\mu_1\mu_2} - k_1^{\mu_2} k_2^{\mu_1}, \quad (4.54)$$

$$T_L^{\mu_1\mu_2} = k_1^2 k_2^2 g^{\mu_1\mu_2} - k_1^2 k_2^{\mu_1} k_2^{\mu_2} - k_2^2 k_1^{\mu_1} k_1^{\mu_2} + k_1 \cdot k_2 k_1^{\mu_1} k_2^{\mu_2}, \quad (4.55)$$

and the form factors are given by

$$\begin{aligned} \tilde{F}_T(k_1, k_2) &= -\frac{1}{\Delta(k_1, k_2)} \left\{ k_{12}^2 (B_0(k_1; m) + B_0(k_2; m) - 2B_0(k_{12}; m)) - 2k_1 \cdot k_{12} k_2 \cdot k_{12} C_0(k_1, k_2; m) \right. \\ &\quad \left. + (k_1^2 - k_2^2) (B_0(k_1; m) - B_0(k_2; m)) \right\} - k_1 \cdot k_2 \tilde{F}_L(k_1, k_2), \end{aligned} \quad (4.56)$$

$$\begin{aligned} \tilde{F}_L(k_1, k_2) &= -\frac{1}{\Delta(k_1, k_2)} \left\{ \left[ 2 - \frac{3k_1^2 k_2 \cdot k_{12}}{\Delta(k_1, k_2)} \right] (B_0(k_1; m) - B_0(k_{12}; m)) \right. \\ &\quad \left. + \left[ 2 - \frac{3k_2^2 k_1 \cdot k_{12}}{\Delta(k_1, k_2)} \right] (B_0(k_2; m) - B_0(k_{12}; m)) \right. \\ &\quad \left. - \left[ 4m^2 + k_1^2 + k_2^2 + k_{12}^2 - 3 \frac{k_1^2 k_2^2 k_{12}^2}{\Delta(k_1, k_2)} \right] C_0(k_1, k_2; m) - 2 \right\}, \end{aligned} \quad (4.57)$$

where  $k_{12} = k_1 + k_2$  and  $\Delta(k_1, k_2) = k_1^2 k_2^2 - (k_1 \cdot k_2)^2$ . As expected the rational and bubble coefficients are identical with the case for a fermion loop. By contracting Eq. (4.55) with currents for the quark-antiquark lines we then arrive at the result for the amplitude. All helicity combinations can be obtained from permutations of the single expression,

$$\begin{aligned} A_4^{4q}(1_{\bar{q}}^+, 2_q^-, 3_{\bar{q}'}^+, 4_{q'}^-; h) &= \left[ \frac{\langle 2|(3+4)|1\rangle \langle 4|(1+2)|3\rangle + \langle 24\rangle [13] (2p_{12} \cdot p_{34})}{s_{12} s_{34}} \right] \tilde{F}_T(p_{12}, p_{34}) \\ &\quad + 2 \langle 24\rangle [13] \tilde{F}_L(p_{12}, p_{34}). \end{aligned} \quad (4.58)$$

## 5 Recap of inclusive and 1-jet results

In this section we briefly review results for the inclusive and 1-jet cases, focussing on understanding the pattern of results observed in the existing literature.

For all the results presented in this paper we consider the LHC operating at  $\sqrt{s} = 14$  TeV and employ the MMHT NLO set [27]. In addition we use a choice of renormalization and factorization scales appropriate for the study of Higgs+multijet events,

$$\mu_f = \mu_r = \frac{H'_T}{2} = \frac{1}{2} \left( \sqrt{m_h^2 + p_{T,h}^2} + \sum_i |p_{T,i}| \right), \quad (5.1)$$

where the sum runs over any jets (equivalently in our case, partons) present. The mass of the top quark is  $m_t = 173.3$  GeV.

### 5.1 Inclusive cross section

From Eq. (2.4) we can abbreviate the form of the SM and SUSY contributions to the amplitude for inclusive Higgs production as,

$$\mathcal{M}^{SM} = \mathcal{H}_2^{gg} = C F_{1/2}(4m_t^2/m_h^2), \quad (5.2)$$

$$\mathcal{M}^{SUSY} = \mathcal{A}_2^{gg}(\tilde{t}_1) + \mathcal{A}_2^{gg}(\tilde{t}_2) = C \left[ \left( \frac{v}{2m_{\tilde{t}_1}^2} \right) \lambda_{h\tilde{t}_1\tilde{t}_1} F_0(4m_{\tilde{t}_1}^2/m_h^2) + \left( \frac{v}{2m_{\tilde{t}_2}^2} \right) \lambda_{h\tilde{t}_2\tilde{t}_2} F_0(4m_{\tilde{t}_2}^2/m_h^2) \right],$$

where  $C$  is a common overall factor that is unimportant for the following argument but which can be identified by comparison with Eq. (2.4). Since we are interested in measuring deviations from the SM result, it is useful to analyze the regions of SUSY parameter space in which these are expected to be small and therefore hard to probe. In order to simplify the argument we will make the simplifying assumption that we can always work in the EFT, i.e. that  $m_t, m_{\tilde{t}_1}, m_{\tilde{t}_2} \gg m_h$ , so that  $F_0$  and  $F_{1/2}$  can be replaced by their asymptotic values. This will be broadly true for the range of parameters in which we are interested but we note that, regardless, the features we elucidate here arise even when this no longer holds. Performing this replacement we arrive at the simple result,

$$\mathcal{M}^{SM} = -\frac{4C}{3}, \quad (5.3)$$

$$\mathcal{M}^{SUSY} = -\frac{C}{3} \left[ \left( \frac{v}{2m_{\tilde{t}_1}^2} \right) \lambda_{h\tilde{t}_1\tilde{t}_1} + \left( \frac{v}{2m_{\tilde{t}_2}^2} \right) \lambda_{h\tilde{t}_2\tilde{t}_2} \right]. \quad (5.4)$$

Since we are working in the limit in which the EFT is valid we can also drop the terms proportional to  $\alpha_1$  and  $\alpha_2$  (since they are suppressed by  $m_Z^2/m_t^2$ ). In that case we have the further simplification of the SUSY amplitude,

$$\mathcal{M}^{SUSY} = -\frac{C}{6} \left[ \left( \frac{m_t^2}{m_{\tilde{t}_1}^2} \right) \left( 2 - \frac{(\Delta m)^2}{2m_t^2} \sin^2 2\theta \right) + \left( \frac{m_t^2}{m_{\tilde{t}_2}^2} \right) \left( 2 + \frac{(\Delta m)^2}{2m_t^2} \sin^2 2\theta \right) \right] \quad (5.5)$$

$$= -\frac{C}{3} \left[ \frac{m_t^2}{m_{\tilde{t}_1}^2} + \frac{m_t^2}{m_{\tilde{t}_2}^2} - \frac{1}{4} \sin^2 2\theta \frac{(\Delta m)^4}{m_{\tilde{t}_1}^2 m_{\tilde{t}_2}^2} \right], \quad (5.6)$$

c.f. Eq. (2.15) of ref. [8].

The form of these amplitudes allows us to anticipate the situations when the SUSY contribution is very small. Due to the mixing allowed in the top quark sector, this can occur when the SUSY amplitude itself vanishes. It is instructive to rewrite Eq. (5.6) as,

$$\mathcal{M}^{SUSY} = \frac{C}{12m_{\tilde{t}_1}^2 m_{\tilde{t}_2}^2} \left[ \sin^2 2\theta (\Delta m)^4 - 4m_t^2 (\Delta m)^2 - 8m_t^2 m_{\tilde{t}_1}^2 \right], \quad (5.7)$$

so that the dependence on  $m_{\tilde{t}_2}$  in the numerator has been eliminated. From this it is clear for which values of  $m_{\tilde{t}_1}$ ,  $\Delta m$  and  $\theta$  the amplitude vanishes, so that the SUSY result is very close to the SM one. Solving for  $\mathcal{M}^{SUSY} = 0$  we find this occurs when ( $\theta > 0$ ),

$$\Delta m = m_t \times \sqrt{2} \times \sqrt{\frac{1 + \sqrt{1 + 2 \sin^2 2\theta} m_{\tilde{t}_1}^2 / m_t^2}{\sin^2 2\theta}}. \quad (5.8)$$

The coincidence of the SM and SUSY cross sections discussed above arises from a vanishing of the SUSY amplitude. In addition, there can be a further coincidence when the effect of interference

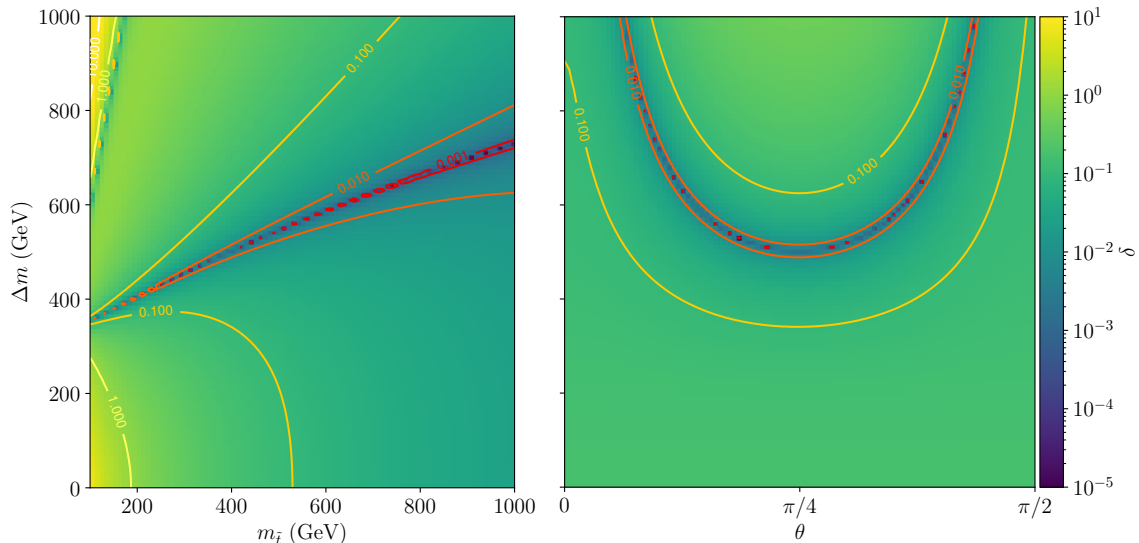


**Figure 2.** The deviation of the inclusive Higgs cross section from the SM case, measured by  $\delta$  defined in Eq. (5.13). The left panel shows  $\delta$  as a function of  $m_{\tilde{t}_1}$  and  $\Delta m$  with top squarks mixing in a maximal fashion ( $\theta = \frac{\pi}{4}$ ). In the right panel  $\delta$  is shown as a function of  $\theta$  and  $\Delta m$ ,  $m_{\tilde{t}_1} = 400$  GeV. In both panels  $\tan \beta = 10$ .

between the SUSY and SM contributions cancels the contribution from the SUSY amplitude squared. In other words we must have an alternative solution when,

$$\begin{aligned} & (\mathcal{M}^{SM} + \mathcal{M}^{SUSY})^2 - (\mathcal{M}^{SM})^2 = 0 \\ \implies & \mathcal{M}^{SUSY} + 2\mathcal{M}^{SM} = 0, \end{aligned} \quad (5.9)$$

Using the results in Eqs. (5.3) and (5.6) we have,

$$\mathcal{M}^{SUSY} + 2\mathcal{M}^{SM} = -\frac{C}{3} \left[ \frac{m_t^2}{m_{\tilde{t}_1}^2} + \frac{m_t^2}{m_{\tilde{t}_2}^2} - \frac{1}{4} \sin^2 2\theta \frac{(\Delta m)^4}{m_{\tilde{t}_1}^2 m_{\tilde{t}_2}^2} + 8 \right]. \quad (5.10)$$

Manipulating as above, we find that this vanishes when,

$$\sin^2 2\theta (\Delta m)^4 - 4(m_t^2 + 8m_{\tilde{t}_1}^2)(\Delta m)^2 - 8m_{\tilde{t}_1}^2(m_t^2 + 4m_{\tilde{t}_1}^2) = 0. \quad (5.11)$$

This equation has no solutions for small  $\Delta m$ . On the other hand, for large  $\Delta m$  the SUSY and SM cross sections are identical when,

$$\Delta m \approx 2 \frac{\sqrt{m_t^2 + 8m_{\tilde{t}_1}^2}}{\sin 2\theta}. \quad (5.12)$$

Again, this solution relies on the existence of a non-zero mixing ( $\theta > 0$ ) between the squarks.

We now turn to a numerical study, measuring the deviation between the SUSY and SM cases by the quantity  $\delta$  defined as [8],

$$\delta = \left| \frac{\sigma^{SM} - \sigma^{SUSY}}{\sigma^{SM}} \right|. \quad (5.13)$$

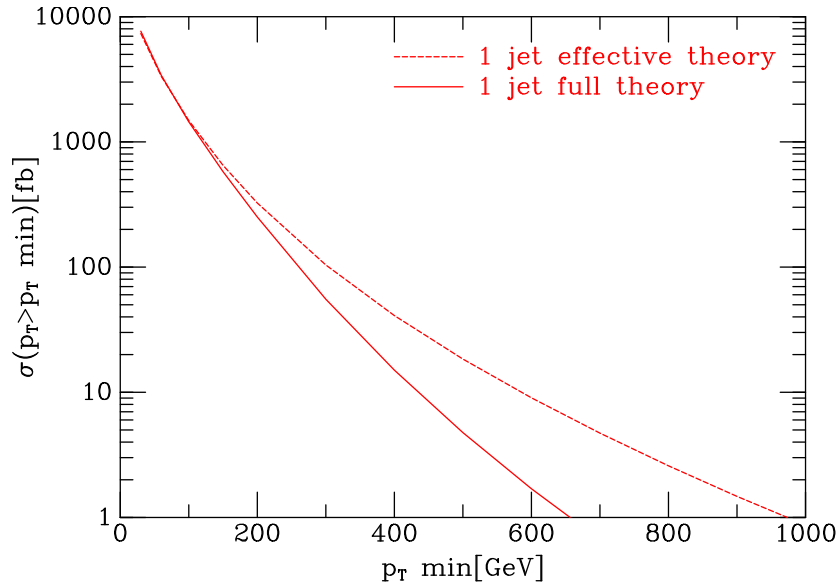


**Figure 3.** Lowest order predictions for H+1 jet in the SM model, computed in the EFT (dashed) and in the full theory (solid).

As discussed above, the case of non-zero mixing is most interesting; in the absence of any mixing the SUSY contribution is simply additive. For this reason we focus on the case of maximal mixing ( $\theta = \pi/4$ ) to illustrate the pattern of behavior. Results for the case  $\tan \beta = 10$ , and as a function of the parameters  $m_{\tilde{t}_1}$  and  $\Delta m$ , are shown in Fig. 2 (left). This figure demonstrates the regions of vanishing  $\delta$  anticipated above. First, the vanishing of the SUSY amplitude occurs, in the maximal-mixing case, for values of  $\Delta m$  given by,

$$\Delta m \approx m_t \sqrt{2 \left( 1 + \sqrt{2} m_{\tilde{t}_1} / m_t \right)}. \quad (5.14)$$

This corresponds to the dark blue stripe across the middle of the plot in Fig. 2 (left), already observed in Ref. [8]. The cancellation at the level of the cross section, i.e. as expected from Eq. (5.12), corresponds to the lighter-blue line in the upper-left corner of the plot. In the region shown,  $m_{\tilde{t}_1} \approx m_t$ , it is approximately given by  $\Delta m \approx 6m_{\tilde{t}_1}$ .

Note that, although we have used asymptotic results for the amplitudes to derive the presence and locations of the features above, these are clearly sufficient to capture the dominant effects. At smaller values of  $m_{\tilde{t}_1}$ , and to some extent  $\Delta m$ , the precise contours of vanishing  $\delta$  vary slightly but are still present.

Although the maximal-mixing case is of highest interest here, as an indication of the effect of a smaller amount of mixing, Fig. 2 (right) shows similar contours as a function of  $\theta$  and  $\Delta m$ , for fixed  $m_{\tilde{t}_1} = 400$  GeV. Again the region of vanishing  $\delta$  that is clearly visible in the figure is easily understood from Eq. (5.8).

## 5.2 1-jet cross section

The case when the Higgs boson is produced in association with a jet has also been discussed extensively in the literature [6–8]. As explained in Ref. [8], the pattern of deviations from the SM is very similar to the inclusive case for low- $p_T$  jets, but begins to differ as the jet (or equivalently, Higgs boson)

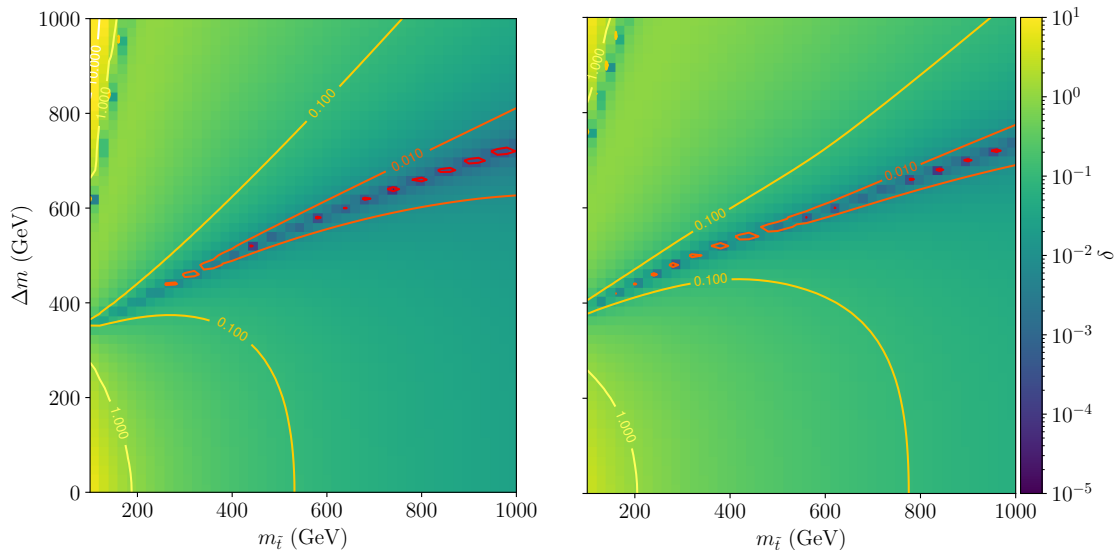


**Figure 4.** The deviation of the Higgs+1 jet cross section from the SM case, measured by  $\delta$  defined in Eq. (5.13), as a function of  $m_{\tilde{t}_1}$  and  $\Delta m$ . Top squarks mix in a maximal fashion ( $\theta = \frac{\pi}{4}$ ) and  $\tan\beta = 10$ . Results are shown for two choices of jet  $p_T$ : 30 GeV (left) and 600 GeV (right).

is produced at large transverse momentum. A simple way to understand this behaviour is in terms of the ability of the jet to resolve the loop of coloured particles, which is demonstrated for the SM case in Fig. 3. To compute the cross sections shown in this figure we have defined jets according to a minimum  $p_T$ , also satisfying the requirement  $|y(\text{jet})| < 2.4$ . As discussed earlier, the calculations in the full theory and in the EFT only begin to differ around  $p_T \sim 200$  GeV, i.e. when the jet is sufficiently energetic to resolve the top-quark loop. The same applies, of course, for the SUSY amplitude, except that the appropriate scales are now set by  $m_{\tilde{t}_1}$  and  $\Delta m$ . In the low- $p_T$  region both the SM and SUSY contributions to the amplitude can be computed in the effective theory and thus the pattern of deviations from the SM must be very similar to the inclusive case. Indeed, since the equality of the SM and SUSY cross sections is tied to the structure of the SUSY amplitude, the  $p_T$  of the jet should be of order  $m_{\tilde{t}_1}$  in order to probe the dependence on the SUSY parameters more effectively.

This argument has been discussed in great detail in Ref. [8], from which we reproduce one set of results in order to illustrate this point. Fig. 4 shows the dependence of  $\delta$  on  $m_{\tilde{t}_1}$  and  $\Delta m$  for the 1-jet process, for two choices of minimum jet (Higgs)  $p_T$ . For the case of a low jet  $p_T$  cut, at 30 GeV (Fig. 4, left panel), the deviations from the SM case are essentially identical to the 0-jet case (c.f. Fig. 2, left). For a much higher cut, at 600 GeV, the jet is able to resolve at least the top quark loop and also the top squark, for values of  $m_{\tilde{t}_1}$  up to a similar scale. This breaks the similarity with the 0-jet case, leading to larger deviations from the SM. This is most visible in the contours of constant  $\delta$ , that are now more constraining for the 1-jet case. This confirms the results presented in Ref. [8].

The region where the lightest top squark is degenerate with the top quark,  $m_{\tilde{t}_1} \approx m_t$ , has received considerable interest due to the difficulty of directly detecting a signal from such a model (see, for instance, Ref. [28] and references therein). Although in general this scenario results in large corrections to the Higgs boson rate, the blue lines in Fig. 2 (left) indicate the two regions where deviations are

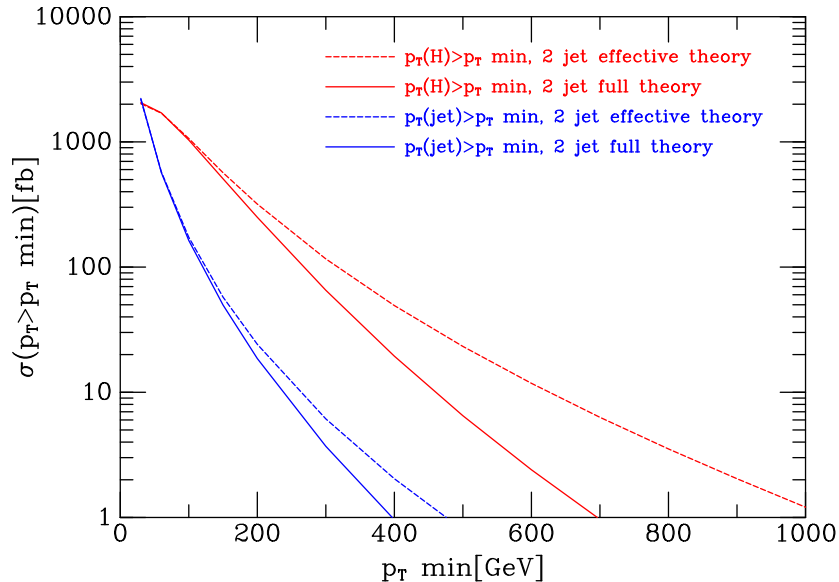


**Figure 5.** Rates for H+2 jet production in the SM, as a function of a minimum  $p_T$ , computed in the full theory (solid) and EFT (dashed). Jets are either subject to this minimum  $p_T$  themselves (blue), or they are only required to satisfy a 30 GeV cut and the minimum  $p_T$  cut is applied to the Higgs boson  $p_T$  (red).

small and an indirect search via the inclusive Higgs cross section is similarly insensitive. However, applying a sufficiently high cut on the transverse momentum of the Higgs boson modifies both of these regions (Fig. 4, right) and such scenarios could be excluded by comparing the 0- and 1-jet rates.

## 6 Results for the 2-jet process

For the 2-jet case we must supplement the jet  $p_T$  and rapidity threshold by a proper jet clustering algorithm. For this we choose the anti- $k_T$  algorithm with a jet resolution parameter  $R = 0.5$ .

As we have already discussed, differences between the pattern of cross-section deviations are intimately connected to the breakdown of the EFT approach to describing these processes. We therefore first examine this for the 2-jet case in the SM, with the results shown in Fig. 5. As the jet  $p_T$  cut is increased, the difference between the EFT and the full theory is not as pronounced in the 2-jet case as in the 1-jet process (comparing blue curves in Fig. 5 with Fig. 3). As explained in Ref. [29], which explored the limitations of the EFT by studying Higgs+1, 2 and 3 jet processes, this is because the breakdown of the EFT is controlled by the  $p_T$  of the single hardest particle in the process. Requiring two very hard jets only serves to decrease the rate without providing an additional probe of the loop-induced Higgs coupling. Therefore, in order to drive the EFT breakdown more efficiently, and thus observe a different pattern of dependence on the SUSY parameters, we should employ a cut that requires a single hard particle. Therefore we choose to cluster jets with the usual cut,  $p_T(\text{jet}) > 30$  GeV, and then make a cut on the  $p_T$  of the Higgs boson. In this case the difference between the full theory and the EFT is very similar in the 1- and 2-jet cases (comparing red curves in Fig. 5 with Fig. 3).

We now use this same cut to explore the breakdown of the EFT for the case of a scalar particle in the loop, with results shown in Fig. 6. For this study we consider only the effect of a single scalar particle in the loop and no top quark, with the amplitudes for the scalar-mediated EFT implemented

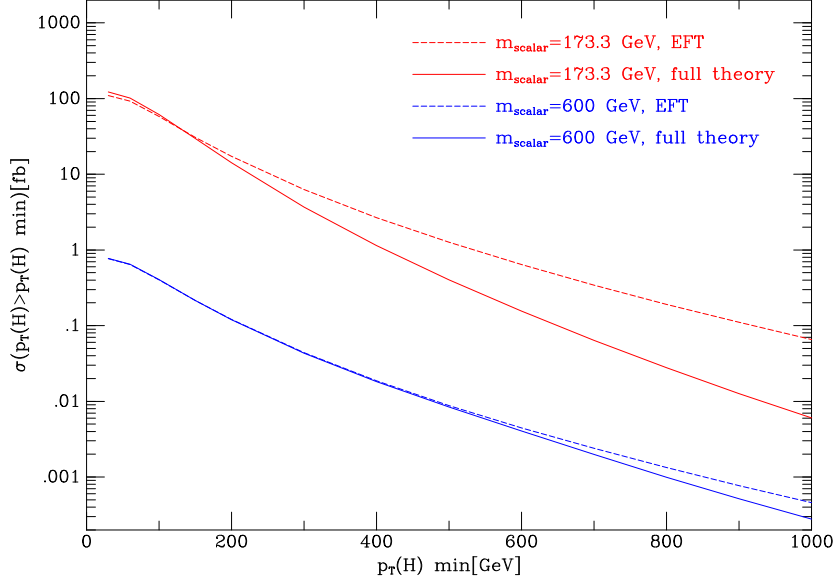


**Figure 6.** Rates for H+2 jet production through a scalar loop, as a function of a minimum  $p_T$  applied to the Higgs boson, computed in the full theory (solid) and EFT (dashed). The scalar mediator mass is either 173.3 GeV (red) or 600 GeV (blue).

according to the discussion in appendix B. For a direct comparison with the fermion case we show results for  $m_{\text{scalar}} = m_t = 173.3$  GeV, and also for a much higher mass,  $m_{\text{scalar}} = 600$  GeV. As expected, for each case the breakdown of the EFT occurs for  $p_T(H, \text{min}) \sim m_{\text{scalar}}$ . As illustrated in Fig. 1, for the inclusive process, the behaviour of the fermionic and scalar amplitudes in the vicinity of the 2-particle threshold differs. However, for the 2-jet case, any such difference is not reflected at the level of the cross-section, as shown in Fig. 7. Although the effective theory appears to work a little better for high  $p_T(\text{min})$  in the scalar case, overall the two curves are very similar. In the limit of small  $p_T(\text{min})$  the result in the full theory is actually larger than the one computed in the EFT, in both cases. This is expected from the inclusive calculation, which these results should resemble as  $p_T(\text{min}) \rightarrow 0$ , where the ratios can be computed from Eqs. (2.5) and (2.6) (c.f. also Fig. 1),

$$\begin{aligned} \sigma^{\text{full}}(gg \rightarrow H)/\sigma^{\text{EFT}}(gg \rightarrow H)|_{\text{fermion}} &= [F_{1/2}(4m_t^2/m_h^2)/(-4/3)]^2 = 1.065, \\ \sigma^{\text{full}}(gg \rightarrow H)/\sigma^{\text{EFT}}(gg \rightarrow H)|_{\text{scalar}} &= [F_0(4m_t^2/m_h^2)/(-1/3)]^2 = 1.157. \end{aligned} \quad (6.1)$$

Although the two curves in Fig. 7 never reach these values, due to the presence of the additional jets, they do reflect this underlying difference in the quality of the EFT.

To examine the sensitivity of the 2-jet process to the SUSY parameters we again focus on the maximal-mixing case. We first assess the dependence on the minimum Higgs  $p_T$  cut that is applied, for the case of  $m_{\tilde{t}_1} = 600$  GeV. The results are shown in Fig. 8. Note that we have covered a range of  $p_T$  that we expect to be accessible at the LHC – the cross-section above 800 GeV is less than 0.5fb, so around 1500 such Higgs events in the full HL-LHC dataset,  $3\text{ab}^{-1}$ . As indicated in the figure, the deviations are bigger in the 2-jet case than for the inclusive cross section. However, the results are almost identical to the 1-jet case, c.f. Fig. 2 of Ref. [8]. This is further reflected in the expected deviations from the SM shown in Fig. 9 – a different pattern from the 0-jet process, but almost identical to the 1-jet results shown in Fig. 4.

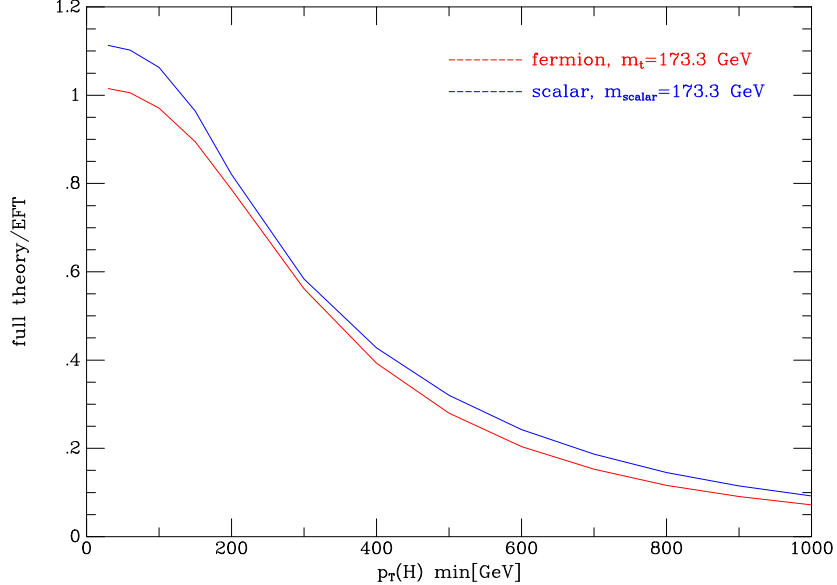


**Figure 7.** The ratio of the cross-section in the full theory to that in the effective theory, for H+2 jet production through a fermion (red) and scalar (blue) loop, as a function of a minimum  $p_T$  applied to the Higgs boson. The mass of the mediator is set to 173.3 GeV in both cases.

## 6.1 Discussion

In evaluating the discriminating power in the 0-, 1- and 2-jet cases above, we have focussed only on the deviations between the rates in the SM and SUSY cases. However, in order to observe such a difference, one must also take into account the number of events that could actually be produced in each case. Reading off the cross-sections from figures 3 and 5 for  $p_T(\text{jet}) > 30$  GeV, and using the (similarly leading-order) result for the inclusive cross-section we have,

$$\begin{aligned}
 \sigma(gg \rightarrow H) &= 16240 \text{ fb}, \\
 \sigma(gg \rightarrow H + 1 \text{ jet}) &= 7640 \text{ fb}, \\
 \sigma(gg \rightarrow H + 2 \text{ jets}) &= 2230 \text{ fb}, \\
 \sigma(gg \rightarrow H + 1 \text{ jet}) &= 2 \text{ fb} \quad (p_T(H) > 600 \text{ GeV}), \\
 \sigma(gg \rightarrow H + 2 \text{ jets}) &= 2 \text{ fb} \quad (p_T(H) > 600 \text{ GeV}).
 \end{aligned} \tag{6.2}$$

Since the number of expected events with a highly-boosted Higgs boson is so small, for both the 1- and 2-jet cases, it appears unlikely that the extra discriminating power could ever come into play. Even accounting for the fact that it may be possible to identify the  $H \rightarrow b\bar{b}$  decay of the Higgs boson in the boosted case – essentially impossible for the bulk of Higgs boson events that occur at low  $p_T$  – the expected event sample would be at least two orders of magnitude smaller than any of the non-boosted ones. In such a case the improved discrimination between the SM and SUSY scenarios would never overcome the loss in statistical power.

Of course, in making this argument we have neglected the role of systematic uncertainties. On the experimental side, the boosted configuration of the Higgs boson means that its decay products are more energetic and thus may be measured with smaller uncertainties. On the other hand, the precision

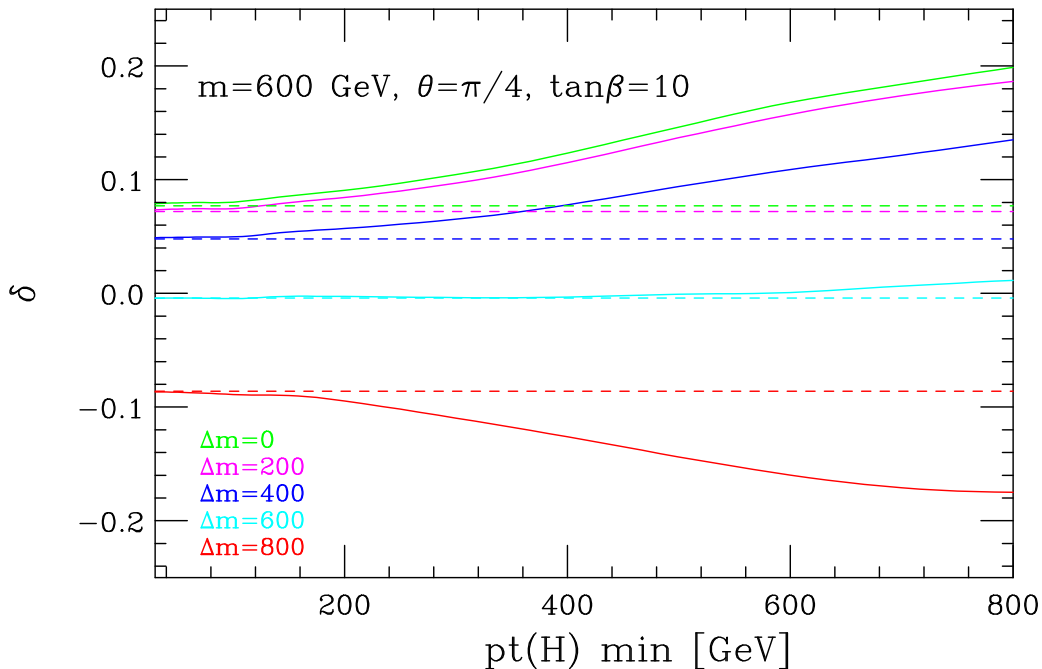


**Figure 8.** 2-jet calculation of  $\delta$  (solid lines), as a function of the cut on the Higgs boson  $p_T$ , for the parameters  $m_{\tilde{t}_1} = 600$  GeV,  $\theta = \frac{\pi}{4}$  and  $\tan\beta = 10$ . The corresponding inclusive result is shown as a dashed line.

of the SM theoretical prediction with which the data must be compared is much reduced: going from current percent-level uncertainties in an expansion up to N<sup>3</sup>LO at the inclusive level [1, 2] to 10% level uncertainties from NNLO in the boosted case [30–34]. While it is clear that Higgs+multijet events offer a different handle on signals of new physics, a proper accounting of both statistical and systematic uncertainties is essential to fully understand their value.

## 7 Conclusions

In this paper we have provided an analytic calculation of all amplitudes representing the scattering of a Higgs boson and four partons, mediated by a loop of color-triplet scalar particles.<sup>1</sup> By combining this with a previous calculation of the corresponding amplitudes in which the mediator particle is a fermion [13] we are able to describe modifications to the SM production of a Higgs boson in association with two jets in theories containing such scalar extensions. As an example we have analyzed the specific case of the MSSM, which contains two relevant scalar particles,  $\tilde{t}_1$  and  $\tilde{t}_2$ . Sensitivity to this scenario has previously been considered extensively in the literature, for both inclusive production and the case of Higgs production in association with one jet. Our study is the first time such an analysis has been performed for the case of two jets.

The results of our calculation show that, although a 2-jet analysis offers improved sensitivity compared to an inclusive analysis, it does not provide an additional benefit over the 1-jet case. This can

<sup>1</sup>A computer-readable form of all the integral coefficients presented in section 4 – which, together with the results in Ref. [13], is sufficient to reproduce these amplitudes – is provided at <https://mcfm.fnal.gov/scalarcoeffs.tar.gz>.

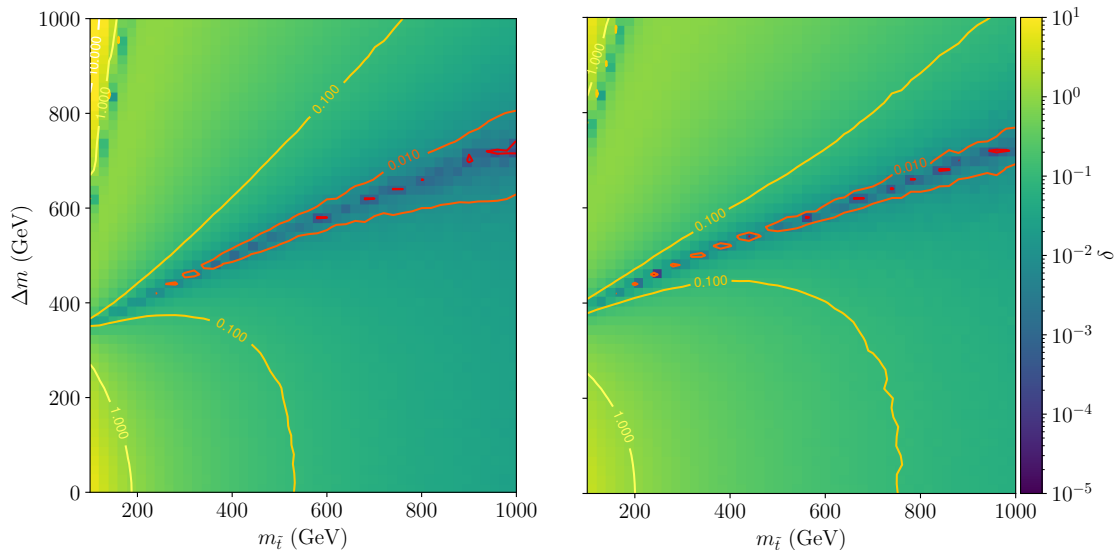


**Figure 9.** The deviation of the Higgs+2 jet cross section from the SM case, measured by  $\delta$  defined in Eq. (5.13), as a function of  $m_{\tilde{t}_1}$  and  $\Delta m$ . Top squarks mix in a maximal fashion ( $\theta = \frac{\pi}{4}$ ) and  $\tan\beta = 10$ . Results are shown in the cases of no additional cut (left) and  $p_T(H) > 600$  GeV (right).

be understood by noting that, in order to probe the nature of the loop process most effectively, the 2-jet analysis should demand only a single hard particle: either a jet, or the Higgs boson itself. In either case the cross section is dominated by configurations in which the Higgs boson recoils against a single hard jet, with the second jet relatively soft. Such configurations are therefore 1-jet-like, with the emission of the second jet well described by the QCD properties of soft and collinear factorization. Moreover, the loss in statistical power that ensues from selecting a sample of events in such a configuration cannot overcome the relatively-small improvement in sensitivity. The same conclusion applies to studies of the 1-jet rate at high transverse momentum.

Finally, we note that if a deviation from the SM prediction were observed in a sample of events containing Higgs bosons produced at high transverse momentum, it would be essential to have precision theoretical predictions for such configurations in a variety of beyond-the-SM scenarios. The amplitudes presented in this paper are an ingredient in a next-to-leading order calculation of the Higgs+jet process in theories containing colour-triplet scalars.

## Acknowledgements

We thank Giuseppe de Laurentis for his input and collaboration in the early stages of this project. The numerical calculations reported in this paper were performed using the Wilson High-Performance Computing Facility at Fermilab and the Vikram-100 High Performance Computing Cluster at Physical Research Laboratory. This document was prepared using the resources of the Fermi National Accelerator Laboratory (Fermilab), a U.S. Department of Energy, Office of Science, HEP User Facility. Fermilab is managed by Fermi Research Alliance, LLC (FRA), acting under Contract No. DE-AC02-07CH11359.

## A Numerical value of coefficients at a given phase-space point

Tables 6 and 7 contain numerical results for the integral coefficients for the  $ggggh$  and  $\bar{q}qggh$  amplitudes respectively, at the phase-space point ( $p = (E, p_x, p_y, p_z)$ )

$$\begin{aligned}
p_1 &= (-15\kappa, -10\kappa, +11\kappa, +2\kappa), \\
p_2 &= (-9\kappa, +8\kappa, +1\kappa, -4\kappa), \\
p_3 &= (-21\kappa, +4\kappa, -13\kappa, +16\kappa), \\
p_4 &= (-7\kappa, +2\kappa, -6\kappa, +3\kappa), \\
p_h &= (+52\kappa, -4\kappa, +7\kappa, -17\kappa),
\end{aligned} \tag{A.1}$$

with  $\kappa = 1/\sqrt{94}$  and  $p_h = -p_1 - p_2 - p_3 - p_4$ . This fixes  $s_{1234} = 25$ ,  $m_h = 5$  and we further choose  $m = 1.5$ .

Due to the correspondence of results between the scalar and fermionic loop cases, many of these values have already been reported in ref. [13]. Tables 6 and 7 therefore contain only the coefficients that differ from the fermionic case.

After including the integrals and rational terms, the values of the colour-ordered subamplitudes are

$$\begin{aligned}
A^{1234}(1^+, 2^+, 3^+, 4^+; h) &= -26.50523303 - 3.722078577 i, & |A^{1234}(1^+, 2^+, 3^+, 4^+; h)| &= 26.76529930, \\
A^{1234}(1^+, 2^+, 3^+, 4^-; h) &= 10.00550042 + 10.39130252 i, & |A^{1234}(1^+, 2^+, 3^+, 4^-; h)| &= 14.42529746, \\
A^{1234}(1^+, 2^-, 3^+, 4^-; h) &= 2.105330472 - 3.500785469 i, & |A^{1234}(1^+, 2^-, 3^+, 4^-; h)| &= 4.085084491, \\
A^{1234}(1^+, 2^+, 3^-, 4^-; h) &= -0.788758613 + 0.151525137 i, & |A^{1234}(1^+, 2^+, 3^-, 4^-; h)| &= 0.803181185.
\end{aligned} \tag{A.2}$$

$$\begin{aligned}
A^{34}(1^+, 2^-, 3^+, 4^+; h) &= -3.151452974 + 5.766222683 i, & |A^{34}(1^+, 2^-, 3^+, 4^+; h)| &= 6.571223621, \\
A^{34}(1^+, 2^-, 3^-, 4^+; h) &= 1.375544184 + 1.088612645 i, & |A^{34}(1^+, 2^-, 3^-, 4^+; h)| &= 1.754194771, \\
A^{34}(1^+, 2^-, 3^+, 4^-; h) &= 3.032201250 - 1.275260855 i, & |A^{34}(1^+, 2^-, 3^+, 4^-; h)| &= 3.289458111.
\end{aligned} \tag{A.3}$$

$$A^{4q}(1^+, 2^-, 3^+, 4^-; h) = 1.583011630 - 1.072246795 i, \quad |A^{4q}(1^+, 2^-, 3^+, 4^-; h)| = 1.911972544. \tag{A.4}$$

## B Large mass limit

Using Eq. (2.2) and the large mass expansion for the scalar triangle integral,

$$C_0(p_1, p_2; m) \rightarrow -\frac{1}{2m^2} - \frac{s}{24m^4} + O\left(\frac{1}{m^6}\right), \quad s = m_h^2 = 2p_1 \cdot p_2, \tag{B.1}$$

we can extract the effective interaction for the fermionic theory,

$$\mathcal{L}_{hgg} = -\frac{1}{4} C_f G_a^{\mu\nu} G_{\mu\nu a} h, \quad C_f = -\frac{g_s^2}{12\pi^2 v}, \tag{B.2}$$

Helicities	Coefficient	Real Part	Imaginary Part	Absolute Value
++++	$\tilde{d}_{1 \times 2 \times 34}$	-0.9840613828	-0.5144323508	1.1104131883
	$\tilde{d}_{1 \times 23 \times 4}$	-3.3548957407	-4.8432206981	5.8916985803
	$\tilde{d}_{1 \times 2 \times 3}$	-6.7445910748	-15.4663942318	16.8730216411
	$\tilde{c}_{1 \times 234}$	-10.6368762164	-31.6829840771	33.4208709592
+++-	$\tilde{d}_{1 \times 2 \times 34}$	23.4451295603	18.5996441921	29.9269254046
	$\tilde{d}_{1 \times 4 \times 32}$	20.5071688388	27.4451393815	34.2604677355
	$\tilde{d}_{2 \times 1 \times 43}$	-4.9009936782	42.1225176136	42.4066767047
	$\tilde{d}_{2 \times 34 \times 1}$	-44.3845463184	-38.3339964812	58.6471076705
	$\tilde{d}_{4 \times 3 \times 21}$	-7.1203811993	0.6886216537	7.1536024635
	$\tilde{d}_{1 \times 23 \times 4}$	-1.8005835535	1.5351129014	2.3661514646
	$\tilde{d}_{2 \times 3 \times 4}$	0.8206155641	1.4735210192	1.6866161680
	$\tilde{d}_{1 \times 2 \times 3}$	-19.2397847846	-1.4762925832	19.2963405429
	$\tilde{d}_{3 \times 4 \times 1}$	-0.3316788675	1.6114692592	1.6452489309
	$\tilde{c}_{4 \times 123}$	-11.0616538761	-1.7916339105	11.2058082504
	$\tilde{c}_{1 \times 234}$	18.9646702722	24.4510167733	30.9436736633
	$\tilde{c}_{2 \times 341}$	-8.9934514290	11.1934355822	14.3588010899
$\tilde{c}_{12 \times 34}$	-3.7461389306	21.0493483972	21.3800988032	
+--+	$\tilde{d}_{4 \times 3 \times 21}$	-6.9368235764	-13.4220769362	15.1086621053
	$\tilde{d}_{1 \times 23 \times 4}$	-5.4005161311	3.8281939917	6.6197162870
	$\tilde{d}_{1 \times 2 \times 3}$	-21.0997803781	-62.3608308275	65.8336840341
	$\tilde{c}_{12 \times 34}$	-39.7403340718	22.2104113517	45.5257786814
	$\tilde{c}_{1 \times 234}$	3.9682125956	13.4813791531	14.0532663489
+---	$\tilde{d}_{1 \times 2 \times 34}$	-0.0267530609	-1.1100908623	1.1104131883
	$\tilde{d}_{1 \times 4 \times 32}$	22.6518970482	-458.1248398611	458.6845074097
	$\tilde{d}_{2 \times 34 \times 1}$	64.2316548189	-59.0233562841	87.2322306708
	$\tilde{d}_{1 \times 23 \times 4}$	-5.7450785528	3.2885735727	6.6197162870
	$\tilde{d}_{1 \times 2 \times 3}$	-10.8954346530	-12.8836471165	16.8730216411
	$\tilde{c}_{23 \times 41}$	1075.3186068541	747.6290891424	1309.6791061854
	$\tilde{c}_{1 \times 234}$	36.8856220760	-309.1172377677	311.3101601314

**Table 6.** Numerical values of coefficients of the  $gggh$  process not already reported in ref. [13] at kinematic point, A.1

valid when  $m_h^2 \ll m^2$ . From Eq. (2.3) the corresponding effective Lagrangian for the scalar loop is,

$$\mathcal{L}_{hgg} = -\frac{1}{4} C_s G_a^{\mu\nu} G_{\mu\nu a} h, \quad C_s = \frac{g_s^2}{24\pi^2 m^2} \left( -\frac{\lambda}{4} \right). \quad (\text{B.3})$$

From these equations we see that,

$$\frac{\left( \frac{m^2}{v} \right) C_s}{\left( -\frac{\lambda}{4} \right) C_f} = -\frac{1}{2}. \quad (\text{B.4})$$

So, in our canonical normalization in which the coupling factors shown on the left-hand side of Eq. (B.4) are extracted, the amplitudes for the fermion- and scalar-mediated cases are related in the large-mass (EFT) limit by a factor of  $-1/2$ . In other words,

$$m^2 A(\dots; h) \rightarrow -\frac{1}{2} m^2 H(\dots; h), \quad (\text{B.5})$$

Helicities	Coefficient	Real Part	Imaginary Part	Absolute Value
+ - + +	$d_{3 \times 21 \times 4}$	370.4335392027	1300.4704659852	1352.1998520434
	$d_{4 \times 3 \times 21}$	0.9220079194	-4.0077609078	4.1124501332
	$c_{12 \times 34}$	-13.7672899406	-4.3871539915	14.4494080313
	$c_{4 \times 123}$	25.1014609317	92.8813584055	96.2134610133
	$c_{3 \times 412}$	67.1532044289	252.1462326711	260.9353857094
+ - - +	$d_{3 \times 21 \times 4}$	20.8960073185	19.9656478672	28.9010417911
	$d_{4 \times 3 \times 21}$	-0.4267971904	-3.8149302668	3.8387301002
	$c_{12 \times 34}$	-9.0987353955	-7.6314351405	11.8754279123
	$c_{4 \times 123}$	1.9450686855	1.9314994054	2.7411643775
+ - + -	$c_{4 \times 123}$	5.2050785566	1.1864337667	5.3385829453

**Table 7.** Numerical values of coefficients of the  $\bar{q}qggh$  process that differ from ref. [13] at kinematic point, A.1.

where the asymptotic forms for the fermion-mediated amplitudes  $m^2 H(\dots; h)$  are given in Appendix B of Ref. [13].

## References

- [1] C. Anastasiou, C. Duhr, F. Dulat, E. Furlan, T. Gehrmann, F. Herzog et al., *High precision determination of the gluon fusion Higgs boson cross-section at the LHC*, *JHEP* **05** (2016) 058 [[1602.00695](#)].
- [2] B. Mistlberger, *Higgs boson production at hadron colliders at  $N^3LO$  in QCD*, *JHEP* **05** (2018) 028 [[1802.00833](#)].
- [3] CMS collaboration, *Measurement of inclusive and differential Higgs boson production cross sections in the diphoton decay channel in proton-proton collisions at  $\sqrt{s} = 13$  TeV*, *JHEP* **01** (2019) 183 [[1807.03825](#)].
- [4] ATLAS collaboration, *Measurement of the properties of Higgs boson production at  $\sqrt{s}=13$  TeV in the  $H \rightarrow \gamma\gamma$  channel using  $139 \text{ fb}^{-1}$  of pp collision data with the ATLAS experiment*, .
- [5] R. Bonciani, G. Degrandi and A. Vicini, *Scalar particle contribution to Higgs production via gluon fusion at NLO*, *JHEP* **11** (2007) 095 [[0709.4227](#)].
- [6] O. Brein and W. Hollik, *Distributions for MSSM Higgs boson + jet production at hadron colliders*, *Phys. Rev. D* **76** (2007) 035002 [[0705.2744](#)].
- [7] C. Grojean, E. Salvioni, M. Schlaffer and A. Weiler, *Very boosted Higgs in gluon fusion*, *JHEP* **05** (2014) 022 [[1312.3317](#)].
- [8] A. Banfi, A. Bond, A. Martin and V. Sanz, *Digging for Top Squarks from Higgs data: from signal strengths to differential distributions*, *JHEP* **11** (2018) 171 [[1806.05598](#)].
- [9] J. R. Espinosa, C. Grojean, V. Sanz and M. Trott, *NSUSY fits*, *JHEP* **12** (2012) 077 [[1207.7355](#)].
- [10] J. Ellis, C. W. Murphy, V. Sanz and T. You, *Updated Global SMEFT Fit to Higgs, Diboson and Electroweak Data*, *JHEP* **06** (2018) 146 [[1803.03252](#)].
- [11] CMS collaboration, *Search for top squark pair production using dilepton final states in pp collision data collected at  $\sqrt{s} = 13$  TeV*, **2008.05936**.
- [12] ATLAS collaboration, *Search for top-squark pair production in final states with one lepton, jets, and missing transverse momentum using  $36 \text{ fb}^{-1}$  of  $\sqrt{s} = 13$  TeV pp collision data with the ATLAS detector*, *JHEP* **06** (2018) 108 [[1711.11520](#)].

- [13] L. Budge, J. M. Campbell, G. De Laurentis, R. K. Ellis and S. Seth, *The one-loop amplitudes for Higgs + 4 partons with full mass effects*, [2002.04018](#).
- [14] S. Dawson, A. Djouadi and M. Spira, *QCD corrections to SUSY Higgs production: The Role of squark loops*, *Phys. Rev. Lett.* **77** (1996) 16 [[hep-ph/9603423](#)].
- [15] J. F. Gunion and H. E. Haber, *The CP conserving two Higgs doublet model: The Approach to the decoupling limit*, *Phys. Rev. D* **67** (2003) 075019 [[hep-ph/0207010](#)].
- [16] R. Britto, F. Cachazo and B. Feng, *Generalized unitarity and one-loop amplitudes in N=4 super-Yang-Mills*, *Nucl. Phys.* **B725** (2005) 275 [[hep-th/0412103](#)].
- [17] D. Forde, *Direct extraction of one-loop integral coefficients*, *Phys. Rev.* **D75** (2007) 125019 [[0704.1835](#)].
- [18] P. Mastrolia, *Double-Cut of Scattering Amplitudes and Stokes' Theorem*, *Phys. Lett.* **B678** (2009) 246 [[0905.2909](#)].
- [19] W. B. Kilgore, *One-loop Integral Coefficients from Generalized Unitarity*, [0711.5015](#).
- [20] S. Davies, *One-Loop QCD and Higgs to Partons Processes Using Six-Dimensional Helicity and Generalized Unitarity*, *Phys. Rev.* **D84** (2011) 094016 [[1108.0398](#)].
- [21] A. Hodges, *Eliminating spurious poles from gauge-theoretic amplitudes*, *JHEP* **05** (2013) 135 [[0905.1473](#)].
- [22] S. Badger, H. Frellesvig and Y. Zhang, *A Two-Loop Five-Gluon Helicity Amplitude in QCD*, *JHEP* **12** (2013) 045 [[1310.1051](#)].
- [23] S. Badger, *Automating QCD amplitudes with on-shell methods*, *J. Phys. Conf. Ser.* **762** (2016) 012057 [[1605.02172](#)].
- [24] H. B. Hartanto, S. Badger, C. Bronnum-Hansen and T. Peraro, *A numerical evaluation of planar two-loop helicity amplitudes for a W-boson plus four partons*, *JHEP* **09** (2019) 119 [[1906.11862](#)].
- [25] G. de Laurentis and D. Maître, *Extracting analytical one-loop amplitudes from numerical evaluations*, *JHEP* **07** (2019) 123 [[1904.04067](#)].
- [26] V. Del Duca, W. Kilgore, C. Oleari, C. Schmidt and D. Zeppenfeld, *Gluon fusion contributions to H + 2 jet production*, *Nucl. Phys.* **B616** (2001) 367 [[hep-ph/0108030](#)].
- [27] L. Harland-Lang, A. Martin, P. Motylinski and R. Thorne, *Parton distributions in the LHC era: MMHT 2014 PDFs*, *Eur. Phys. J. C* **75** (2015) 204 [[1412.3989](#)].
- [28] T. Cohen, S. Majewski, B. Ostdiek and P. Zheng, *On the ATLAS Top Mass Measurements and the Potential for Stealth Stop Contamination*, *JHEP* **06** (2020) 019 [[1909.09670](#)].
- [29] N. Greiner, S. Höche, G. Luisoni, M. Schönherr and J.-C. Winter, *Full mass dependence in Higgs boson production in association with jets at the LHC and FCC*, *JHEP* **01** (2017) 091 [[1608.01195](#)].
- [30] X. Chen, T. Gehrmann, E. W. N. Glover and M. Jaquier, *Precise QCD predictions for the production of Higgs + jet final states*, *Phys. Lett.* **B740** (2015) 147 [[1408.5325](#)].
- [31] X. Chen, J. Cruz-Martinez, T. Gehrmann, E. W. N. Glover and M. Jaquier, *NNLO QCD corrections to Higgs boson production at large transverse momentum*, *JHEP* **10** (2016) 066 [[1607.08817](#)].
- [32] W. Bizon, X. Chen, A. Gehrmann-De Ridder, T. Gehrmann, N. Glover, A. Huss et al., *Fiducial distributions in Higgs and Drell-Yan production at N<sup>3</sup>LL+NNLO*, *JHEP* **12** (2018) 132 [[1805.05916](#)].
- [33] R. Boughezal, F. Caola, K. Melnikov, F. Petriello and M. Schulze, *Higgs boson production in association with a jet at next-to-next-to-leading order*, *Phys. Rev. Lett.* **115** (2015) 082003 [[1504.07922](#)].
- [34] J. M. Campbell, R. K. Ellis and S. Seth, *H + 1 jet production revisited*, *JHEP* **10** (2019) 136 [[1906.01020](#)].